Precambrian Research 305 (2018) 197–217

Contents lists available at ScienceDirect

Precambrian Research

journal homepage: www.elsevier.com/locate/precamres

The Neoproterozoic evolution of the western Siberian Craton margin: U-Pb-Hf isotopic records of detrital zircons from the Yenisey Ridge and the Prisayan Uplift

Nadezhda Priyatkina[a,b,*], William J. Collins[a,c], Andrei K. Khudoley[d], Elena F. Letnikova[e], Hui-Qing Huang[f]

[a] New South Wales Institute of Frontiers Geoscience, University of Newcastle, Newcastle, NSW 2308, Australia
[b] Laboratory of Main Magnetic Field and Paleomagnetism, Institute of the Earth Physics (IFZ RAN), Moscow, Russia
[c] Department of Applied Geology, Curtin University, GPO Box U198, Perth, WA 6845, Australia
[d] Institute of the Earth Sciences, St. Petersburg State University, 7/9 University Nab., St. Petersburg 199034, Russia
[e] V.S. Sobolev Institute of Geology and Mineralogy, Siberian Branch of the Russian Academy of Science, pr. Koptyuga 3, Novosibirsk 630090, Russia
[f] EGRU, College of Science and Engineering, Division of Tropical Environments and Societies, James Cook University, Townsville, Australia

ABSTRACT

We present new LA ICP-MS U-Pb-Hf detrital zircon data from Neoproterozoic sedimentary basins located along the south-western margin of the Siberian Craton. In the Yenisey Ridge (the Taseeva basin), siliciclastic sedimentary units contain abundant 2.7–2.5 Ga, 2.0–1.75 Ga and 0.95–0.57 Ga detrital zircon populations, whereas for the Prisayan Uplift slightly different detrital zircon ages of 3.0–2.5 Ga, 2.2–1.8 Ga and 0.95–0.65 Ma are common. Mid Neoproterozoic sandstones were deposited in a rift setting or along a rifted cratonic margin facing a back-arc basin, whereas the immature to submature upper Ediacaran to Lower Cambrian fluvial successions were probably deposited in the foredeep setting, at the expense of proximal Neoproterozoic igneous suites and the underlying metasedimentary basement. A range of εHf values from −10 to +14 indicates intense mixing between juvenile and evolved magma components in a continental arc setting at ca. 950–570 Ma. Geological evidence, persistent input of detrital zircon material derived from ancient crustal units of western Siberian cratonic margin and evolution of Hf isotopic compositions suggest that the Neoproterozoic arc system of the Yenisey Ridge and, partly, Sayan orogens developed along the active margin of Siberia. In the Neoproterozoic, the arc system probably extended along the periphery of Rodinia into the Taimyr orogen of northern Siberia and Valhalla orogen of north-eastern Laurentia.

1. Introduction

Global Neoproterozoic geodynamics and continental drift is the significant question of modern geoscience (e.g., Cawood et al., 2016; Johansson, 2014; Li et al., 2013; Merdith et al., 2017). Information about the Neoproterozoic interactions between cratonic landmasses can be gained from Neoproterozoic orogenic belts of poorly studied cratonic margins, such as those of the Siberian Craton (SC).

The Neoproterozoic crust is widespread along the western fringe of the SC, where the orogenic belt of the Yenisey Ridge (Fig. 1) incorporates granitoids and arc-related volcanic rocks, covering an age range of at least 860–550 Ma (e.g., Vernikovsky et al., 2003, 2009 and ref. therein; see Fig. 2a). Younging towards the west, the orogenic belt makes up the Isakovka-Predivinsk (IPT) and the Central Angara terrane (CAT), thrusted onto the Mesoproterozoic sedimentary succession of the SC, namely the East Angara terrane (EAT, Vernikovsky et al., 2003).

Neoproterozoic igneous and metamorphic suites of similar age occur also in the north-western East Sayan (Bezzubtsev and Perfilova, 2008; Nozhkin et al., 2007, 2015b; Turkina et al., 2004, 2007), which forms an apparent extension of the Yenisey Ridge orogen (Fig. 1). The Meso- to Neoproterozoic terranes and fragments of the early Precambrian basement such as the Biryusa and the Angara-Kan terranes collectively form the north-western East Sayan. The south-eastern East Sayan is separated from the north-western East Sayan by a megathrust and appears to represent a separate crustal ribbon, which together with Neoproterozoic crust of the Tuva-Mongolia and the Dzavhan block forms an oroclinal structure that extends into the Tian-Shan orogen as part of the Central Asian Orogenic Belt (Buslov et al., 2013; Dobretsov

* Corresponding author at: New South Wales Institute of Frontiers Geoscience, University of Newcastle, Newcastle, NSW 2308, Australia.
E-mail address: nadezda.priyatkina@uon.edu.au (N. Priyatkina).

https://doi.org/10.1016/j.precamres.2017.12.014
Received 31 July 2017; Received in revised form 30 November 2017; Accepted 4 December 2017
Available online 06 December 2017
0301-9268/

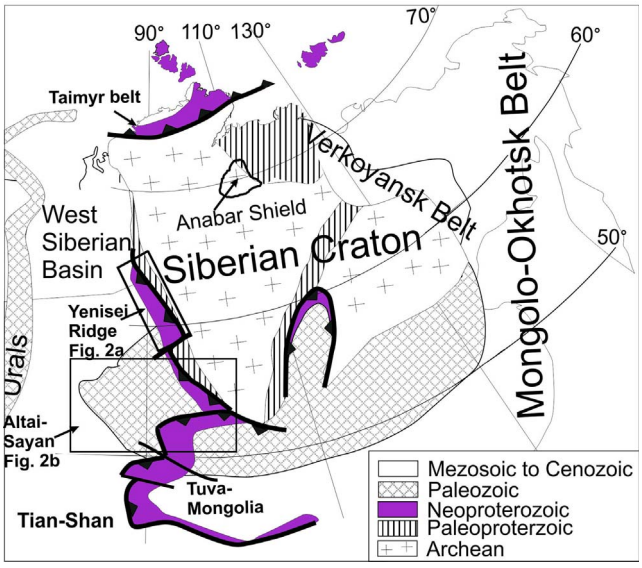

Fig. 1. Location of Neoproterozoic crust relative to the Siberian Craton (SC). Archean and Paleoproterozoic of the SC after Rosen et al. (1994).

and Buslov, 2007; Kuzmichev and Larionov, 2011). To the west of north-western East Sayan the Neoproterozoic rocks lapse beneath the Paleozoic subduction-accretion complexes of Kuznets and Gorny Altai (Figs. 1 and 2b).

The Proterozoic evolution of the western SC margin is ambiguous because the cratonic affinity of the Neoproterozoic crust presently located near western SC is uncertain (Kuzmichev and Sklyarov, 2016; Vernikovsky et al., 2009, 2016) and the presence of an ophiolitic suture between the EAT and CAT (discussed in Nozhkin, 2009; Vernikovsky et al., 2009) is questionable. On one hand, it is known that Neoproterozoic crustal ribbons of peri-Gondwanan origin accreted to Siberia in the Paleozoic times (Abrajevitch et al., 2008; Buslov et al., 2001; Kröner et al., 2014; Levashova et al., 2011; Rojas-Agramonte et al., 2011). On the other hand, the widespread angular late Neoproterozoic unconformity that extends from CAT into the Siberian platform provides evidence for a major orogenic event along the western margin of Siberia at the end of Neoproterozoic, consistent with the idea of active Neoproterozoic SC margin (Buslov et al., 2013; Metelkin et al., 2012).

Vernikovsky et al. (2003, 2009) suggest that a set of two collisional events resulted in formation of the Yenisey orogen near the western SC margin, so that the collision of the CAT and the SC at ~850 Ma followed by collision of the IPT with CAT ~650 Ma can be collectively seen as accretionary orogenesis. Furthermore, Kuzmichev and Sklyarov (2016) emphasize the significance of extensional tectonics in between the two contractional events. However, recently Vernikovsky et al. (2016) argued for an exotic origin of the CAT, which requires a much more complex geodynamic model. By contrast, Likhanov et al. (2014) and Nozhkin et al. (2011) see the development of the Yenisey Ridge orogen as a result of a craton-wide collisional event at ~1.0–0.95 Ga, followed by intracratonic rifting, Atlantic style rifting, or rifting associated with arc accretion. As the relationship between the Neoproterozoic arc-related suites and the basement of the SC has not been established, the concepts compete against each other to establish geological evolution of the Yenisey Ridge, East Sayan orogenic belts and the western SC margin in general. In an attempt to resolve the existing controversies and provide a comprehensive model for the formation of the Neoproterozoic crust along the western SC cratonic margin, we investigate the age and magma sources of the erosional products derived from the orogenic belts into the late Neoproterozoic sedimentary basins of western SC.

2. Overview of the analytical procedures

A full description of the analytical procedures used in this study is presented in Supplementary file 1. U-Pb-Hf detrital zircon analyses were guided by CL and transmitted light imaging. LA-ICP-MS U-Pb analyses (Supplementary file 2) were carried out at the University of Newcastle, Australia using a NWR UP-213 Nd:YAG laser ablation system, coupled with an Agilent 7700 ICP-MS. For constructing age probability distribution plots and further interpretation the analyses with discordance greater than 10% and those that plot off the concordia were manually filtered, and to avoid usage of Hf in zircon isotopic data, which age has been reset, $^{177}Hf/^{176}Hf$ ratio has been plotted against the U-Pb age (Figs. 5, 7, 9–11). Also, the analyses with internal errors greater than 3% and propagated errors greater than 5% have been excluded as they most likely reflect heterogeneous isotope ratios of zircons. In Supplementary file 2, the data are presented with propagated errors (2σ), i.e., the errors that also incorporate correction for instrumental drift. $^{206}Pb/^{238}U$ ages are used when grains are younger than 1000 Ma. Otherwise, $^{207}Pb/^{206}Pb$ ages are used as the best estimate of the age of zircon crystallization ages. For the analysed samples we commonly present estimate of maximum depositional age (MDA) based on mean age of the youngest cluster ($n \geq 3$) of grain ages that overlap in age at 2σ, further referred to as mean age of the youngest cluster, as suggested by Dickinson and Gehrels (2009). However, possible implications of young single grain ages are also discussed.

Hf in zircon analyses were carried out in the advanced Analytical Centre at James Cook University, Townsville (Australia) using a GeoLas 193-nm ArF laser and a Thermo Scientific Neptune multicollector ICPMS. In the Supplementary file 2, Hf in zircon data are linked to each U-Pb single grain analysis. .

3. Yenisey Ridge

3.1. Geological setting of the studied sedimentary units

The orogenic belt of the Yenisey Ridge is subdivided into four main structural domains (Fig. 2a), namely the East Angara Terrane (EAT), the Central Angara Terrane (CAT), the Isakovka-Predivinsk Terrane (IPT) and the Angara-Kan Terrane (AKT) (Vernikovsky et al., 2003). The EAT represents a fragment of Mesoproterozoic Siberian continental slope, the CAT and IPT represent Neoproterozoic magmatic arcs and the AKT preserves Paleoproterozoic crust of the Siberian cratonic basement (Nozhkin, 2009; Vernikovsky et al., 2009). The studied samples of the Yenisey Ridge were collected from the Irkineeva Uplift, which forms a part of the EAT.

The Irkineeva Uplift represents a ~70 km × 25 km anticlinal fold, bounded by a set of north-northeasterly oriented late Paleozoic faults (Fig. 3). The core of the anticline comprises the Proterozoic sedimentary succession that broadly can be subdivided into two main sedimentary cycles (Melnikov et al., 2005; Semikhatov and Serebryakov, 1983; Shenfil', 1991). The lower sedimentary cycle is represented by the siliciclastic Sukhopit and the carbonate-dominated Tungusik groups (~1650 (?)–900 Ma, Shenfil', 1991; Volobuev et al., 1976). Its thickness varies from only ~3 km in the study area to ~6–8 km in the CAT and the IPT. In the study area the Tungusik Group is unconformably overlain by the ~200 m thick Krasnogor Formation of feldspar-bearing chlorite-sericite schist (~850 Ma, Galimova et al., 2012). A range of seismic and geological profiles across the Yenisey Ridge (Filippov, 2017; Grazhdankin et al., 2015; Khabarov and Varaksina, 2011; Kheraskova et al., 2009; Melnikov et al., 2005) highlight an unconformity surface, which extends across the Yenisey Ridge eastwards into the Siberian platform. The upper sedimentary cycle is represented by the 3 km thick fluvial succession of the Taseeva Group. It is traditionally subdivided into three conformable siliciclastic formations including the Aleshino, the Chistyakova and the Moshakova (Figs. 3 and 4). The top of the Moshakovka Formation is truncated by an erosional

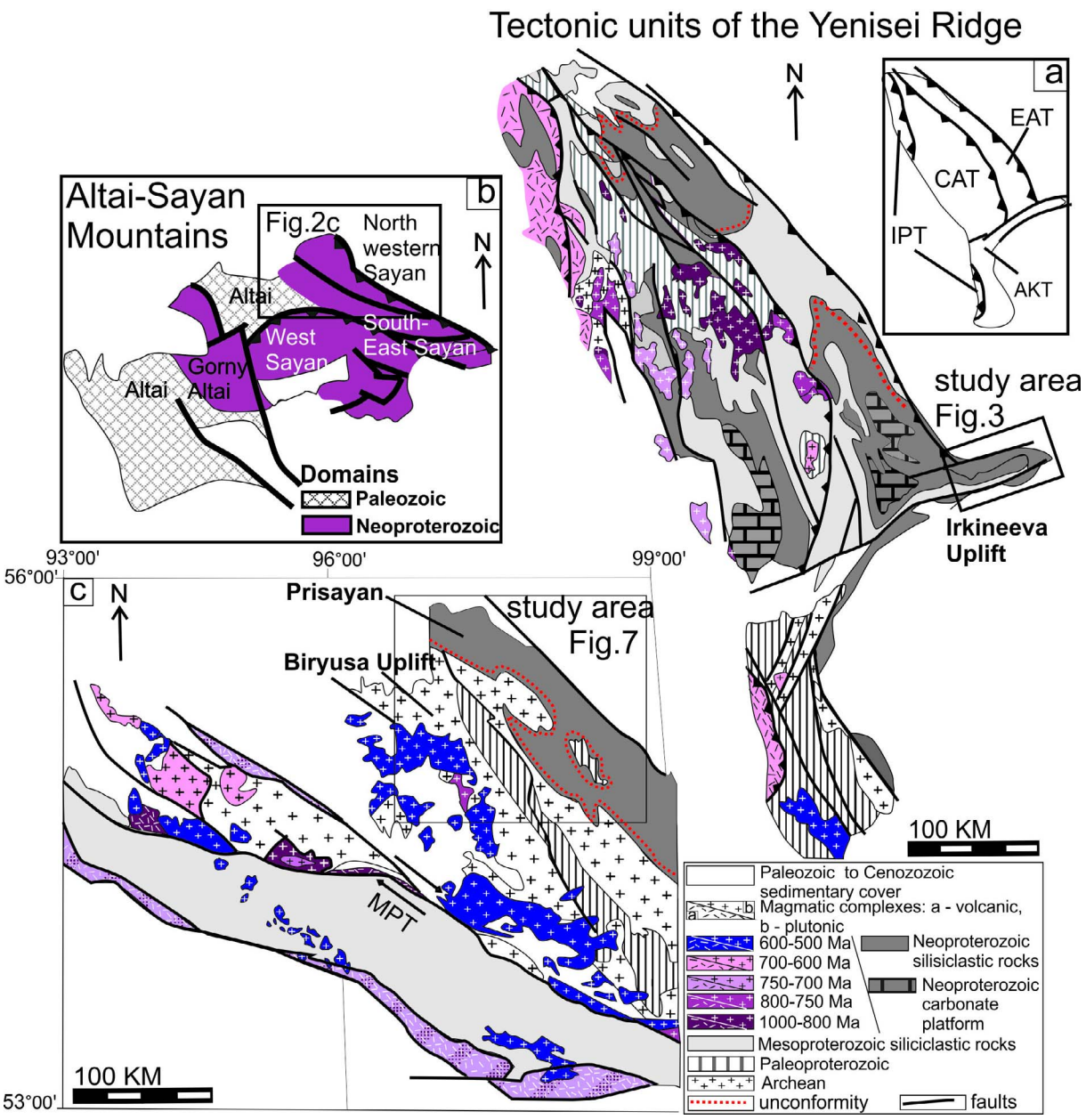

Fig. 2. (a) Geology of the Yenisey Ridge simplified after Nozhkin (2009), Vernikovsky et al. (2009), (2016); (b) Tectonic subdivision of the Altai-Sayan orogenic belt after Postnikov and Terleev (2004); (c) Geology of the Prisayan Uplift, north-western East Sayan, modified after Turkina et al. (2007) using recent geochronological data from Bezzubtsev et al. (2008a), Galimova et al. (2012) and references therein. EAT = East Angara Terrane; CAT = Central Angara Terrane; IPT = Isakovka-Predivinsk Terrane; AKT = Angara-Kan Terrane; MPF = Main Prisayan Fault.

surface, upon which rest the red beds of the Redkoles Formation (~150 m thick in the Irkineeva Uplift), sometimes included into the Taseeva Group (Sovetov et al., 2007; Vernikovsky et al., 2009). Several lines of paleontological (Kochnev and Karlova, 2010; Liu et al., 2013) suggest that the Redkoles units have been deposited during the Nemakit-Daldynian (542–534 Ma), whereas the lower units appear to be slightly older (~555–549 Ma; Liu et al., 2013).

3.2. Description of sampled rock units

The thickness of the lowermost Aleshino Formation in the study area is about ~340 m (Kirichenko et al., 2012; Zuev and Perfilova, 2012). Sovetov and Blagovidov (2004), Sovetov et al. (2007) identified a number of fluvial system components within the formation, such as meandering channels, deltaic fans, lateral accretion bars, overbank deposits and crevasses. Microscopically, the sandstone members consist of cherry-red quartzose to arkosic sandstone (content of quartz is > 90%), interbedded with siltstone and minor conglomerate and shale. In the upper part of the formation quartz arenite is abundant (Kirichenko et al., 2012). It is exemplified by the sample 3-EB-1 of medium grained sublithic quartz arenite. The framework (100%) is well sorted, consists of subrounded monocrystalline quartz grains (~90%), indicating long transportation or intense recycling of the sediment, and rounded fragments of chlorite schist (~10%), indicating relative proximity of some minor sources of clastic material to the depositional area.

Another sampled unit was the Moshakova Formation. It forms the upper part of the Taseeva succession and in the study area it is only ~100 m thick. Sedimentary textures show that the Moshakova Formation rocks are fluvial, mixed with interchannel sandstone and siltstone (Sovetov et al., 2007). The formation is dominated by variegated shale, dolostone, and arkosic sandstone with feldspar content

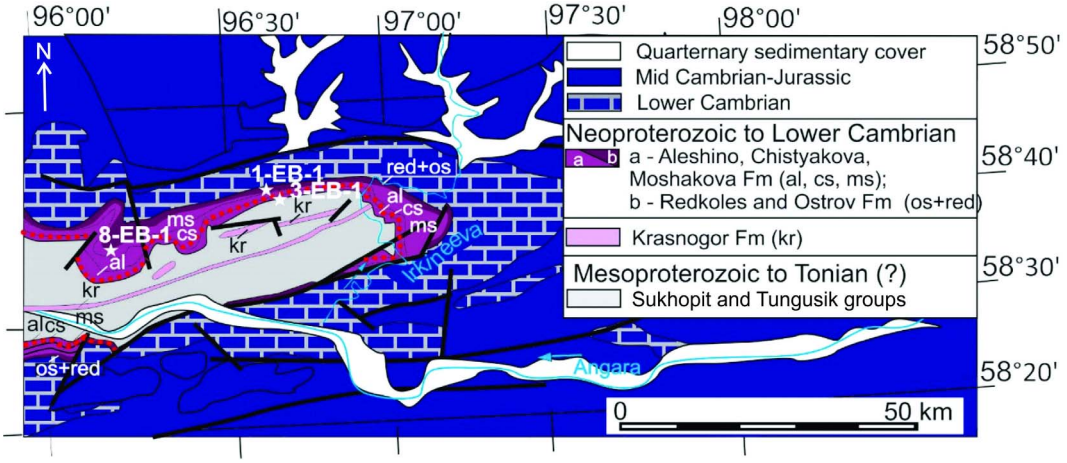

Fig. 3. Geological map of the Irkineeva Uplift showing relationship between the studied units and the sampling locations, simplified after Kovrigina et al. (1974), Zuev and Perfilova (2012).

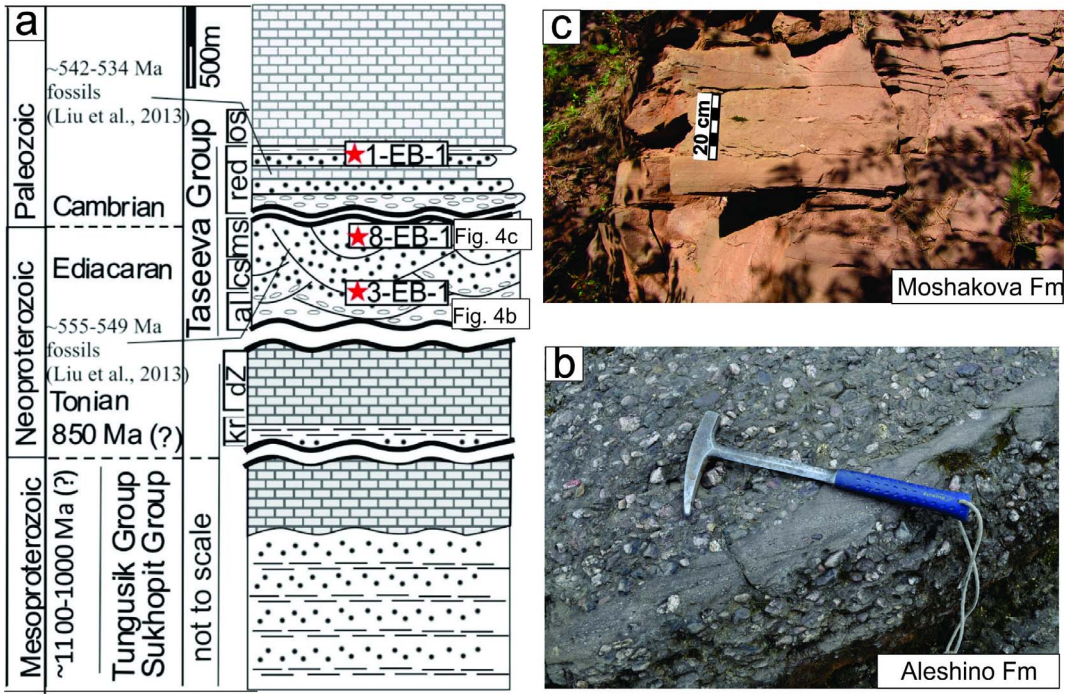

Fig. 4. Simplified stratigraphy of the Neoproterozoic rocks from the Irkineeva Uplift and underlying metasedimentary units compiled from (Berezii et al., 1973; Kirichenko et al., 2012) and the position of sampled rock units. kr = Krasnogor Formation, dz = Dashkino Formation; al = Aleshino Formation; cs = Chistyakova Formation; ms = Moshakova Formation; red = Redkoles units; os = Ostrovnaya Formation.

up to 30% (Kirichenko et al., 2012). Sample 8-EB-1 is represented by medium grained arkose. The framework (100% of the area) consists of moderately to poorly sorted subangular quartz grains (~75%), of which the majority is monocrystalline, although some grains exhibit interlocking textures. ~25% of the framework is represented by feldspar, including altered calcic plagioclase and microcline, suggesting derivation of the sedimentary rock from a local provenance. Trace clinopyroxene and zircon are present.

The overlying Redkoles units belong to the Redkoles-Ostrovnaya Formation of fluvial red sandstone and siltstone, topped by dolostone (Fig. 4). The sandstones are represented by lithic arenites, rich in metasedimentary rock fragments, as well as sub-arkosic varieties with average feldspar content of ~10–15% (Kirichenko et al., 2012; Zuev and Perfilova, 2012). Typical of the Redkoles units, the studied sample 1-EB-1 is classified as sub-lithic sandstone in which subangular, poorly sorted rock and grain fragments indicate that the provenance area was located in the vicinity of the deposition area. The framework (100%) is dominated by monocrystalline quartz grains (70%). The remaining constituents are siltstone (~20%), feldspar including both K-feldspar and plagioclase (~5–10%), rare hornblende and opaque minerals (< 5%).

3.3. Results of U-Pb and Lu-Hf analysis

The samples 3-EB-1, 8-EB-1 collected from the Taseeva Group and 1-EB-1 from the Redkoles units were imaged and analysed for U-Pb-Hf isotopes (Figs. 5 and 6). The sample 3-EB-1 had 104 grains analysed (Supplementary file 2), of which 103 met the 10% discordance criteria (103/104); the sample 8-EB-1 (Moshakova Formation) and the sample 1-EB-1 (Redkoles Formation) yielded 75/93 and 125/150 suitable for further interpretation results, respectively. The majority of filtered analysis plot on the concordia, excluding a few data points that plot

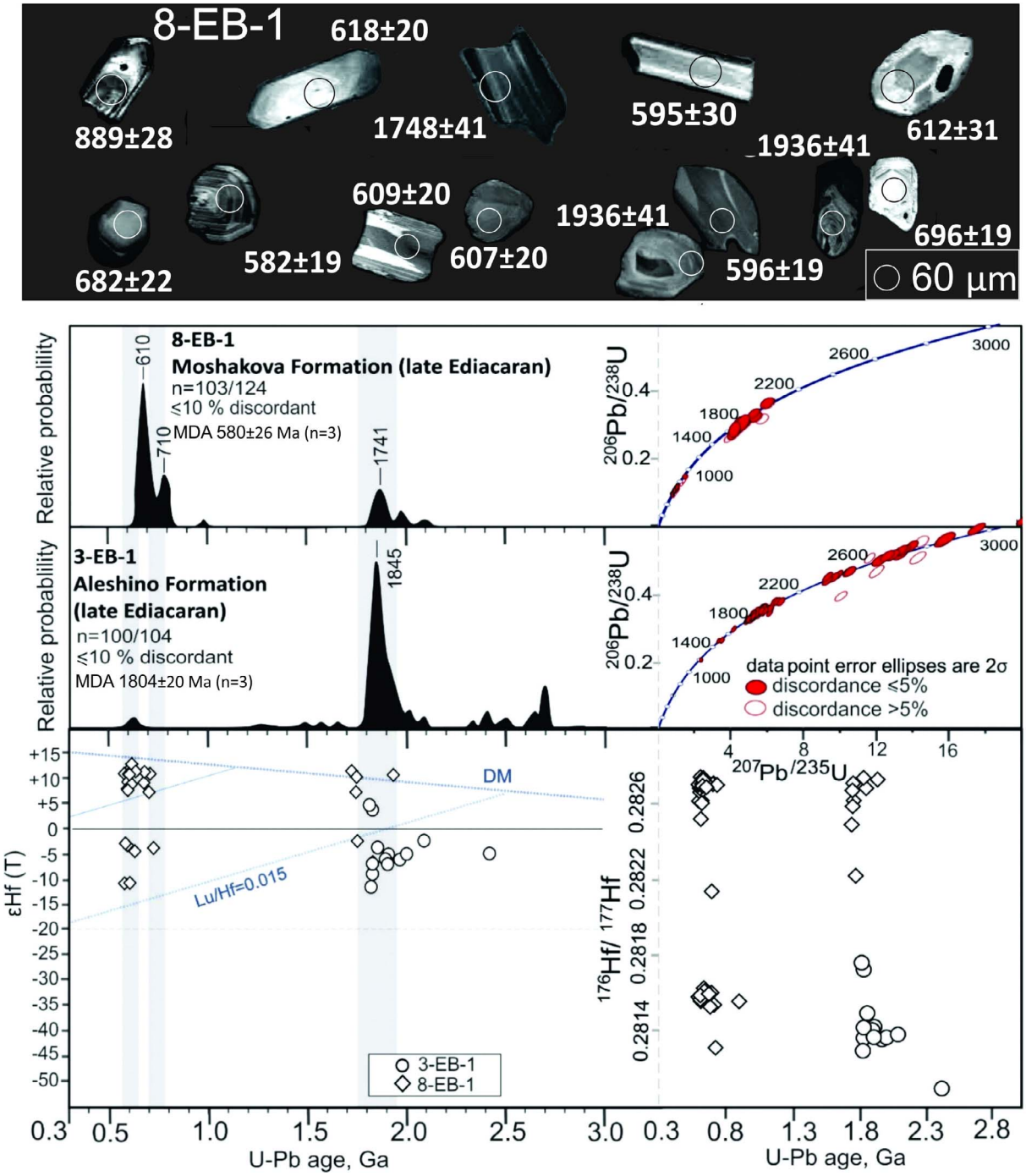

Fig. 5. Age spectra, concordia plots, εHf (T) versus age and $^{177}Hf/^{176}Hf$ ratio versus age of detrital zircon populations for the Taseeva Group, supported by CL images of selected grains.

near concordia. The latter are characterised by $^{207}Pb/^{206}Pb$ ages of 1800–1700 Ma. The samples reveal both morphologically and chronologically different detrital zircon populations.

Zircons from the sample 3-EB-1 are predominantly rounded (Fig. 5). Most of them have Archean to Paleoproterozoic ages (Fig. 5). In the sample, the 1950–1800 Ma zircon population that defines major peak at ca. 1845 Ma is strongly predominant (63%). Some recovered zircons (22%) have Archean ages, covering the 3000–2400 Ma interval of the age spectrum (Fig. 5). The remaining zircons yield late Neoproterozoic, late and early mid-Paleoproterozoic ages. The MDA of the formation based on the mean age of the youngest cluster is 1804 ± 20 Ma (n = 3), which is more than 1 Ga older than the age of sedimentation. Only a few grains of Mesoproterozoic and Ediacaran age (609 ± 12 Ma) are present in this sample.

However, the Neoproterozoic grains are widespread (30% in 1-EB-1 to 75% in 8-EB-1) in the Moshakova Formation and the Redkoles units, and form two clusters near 760–710 Ma and 650–610 Ma (Figs. 5 and 6). The Redkoles units also bears the 970–820 Ma zircon population, which was not identified in the other samples. In both samples, the Neoproterozoic grains are euhedral and often preserve facets (Figs. 5 and 6), suggesting they underwent little transport from the source Neoproterozoic rocks to the basin of sedimentation. The remainder of the total zircon population is represented by late Paleoproterozoic grains, which ages define a probability density peak at ca. 1741 Ma (in sample 8-EB-1), or at ca 1850 Ma (in sample 1-EB-1) similar to that identified in sample 3-EB-1. Sample 1-EB-1 also bears significant

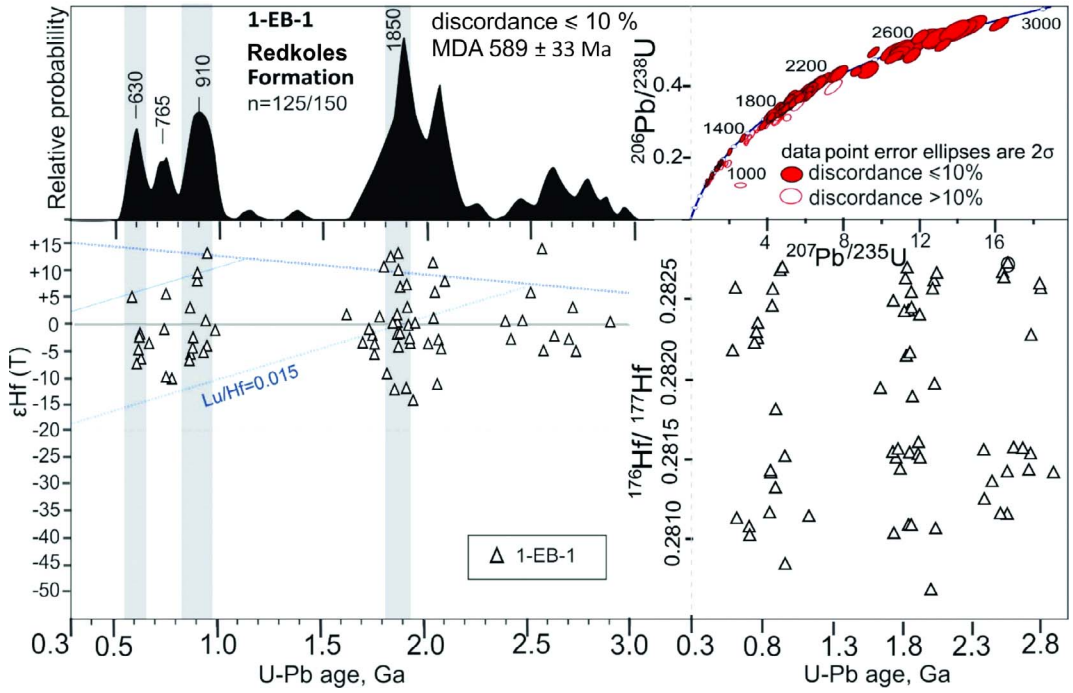

Fig. 6. Age spectra, concordia plots, εHf (T) versus age and $^{177}Hf/^{176}Hf$ ratio versus age of detrital zircon populations for the Redkoles Formation, supported by CL images of selected grains.

amount of grains, which ages fall in ranges of 2150–2000 Ma and 3000–2400 Ma. The MDAs of the Moshakova and Redkoles formations based on the mean age of the youngest cluster (n = 3) correspond to 586 ± 20 Ma and 589 ± 33 Ma, resembling previously assumed ages of deposition.

The ca. 2100–1950 Ma zircons in both samples 8-EB-1 (Fig. 5) and 1-EB-1 (Fig. 6) are characterised by εHf (T) values of −5 to +10, corresponding to Hf model ages that range between 3000 Ma and 2150 Ma. The abundant in the samples 3-EB-1 and 1-EB-1 ca. 1850 Ma zircon population shows a greater variety of εHf (T) values from +5 to −15 with a density maximum localized between −10 and 0. εHf (T) of younger Paleoproterozoic grains (1800–1700 Ma) is different in samples 8-EB-1 and 1-EB-1. In the sample 8-EB-1 four analysed zircon grains are juvenile, with εHf (T) in range of +10 to +15. The majority of εHf (T) at 1800 Ma data points from sample 1-EB-1 fall in range between −7 and +1. Thus, rather than building the vertical array in Hf vs age space, the 1800–1750 Ma zircons form two distinct clusters.

4. Biryusa-Prisayan Uplift

4.1. Geological setting of the studied sedimentary units

Another studied sedimentary succession forms ~4–6 km thick predominantly fluvial sedimentary fill of the Prisayan Uplift (sometimes also referred to as the Pri-Sayan, the Pre-Sayan or the Sayan foredeep), located in the south-western margin of the Siberian Craton. It represents a several hundred km long north-westerly trending asymmetrical megascale fault-bend fold (Fig. 2). Locally, the Prisayan basinal fill unconformably rests above the Archean and Paleoproterozoic basement rocks of the Biryusa Uplift, but dominantly they have faulted contacts (Fig. 7). The Biryusa Uplift comprises the Paleoproterozoic Neroi and Subluk metasedimentary and metavolcanosedimentary units, intruded by the Sayan granitic intrusions during two main phases, ca. 1870 and ca. 1734 Ma, and minor Archean units (e.g., Donskaya et al., 2014; Turkina et al., 2006). The suite forms a part of a larger granitoid belt that outlines western Siberian margin as part of the Angara Fold Belt (Rosen et al., 1994). In the northeast, the structure of Prisayan Uplift flattens beneath the Paleozoic platform cover. In the south (outside the study area), the Prisayan basinal succession overlies the Mesoproterozoic Urik-Iya graben fill (Galimova et al., 2012). The Neoproterozoic arc-related suites occur beyond the south-western extents of the Biryusa block and the Urik-Iya graben.

The Neoproterozoic to Lower Cambrian succession of the Prisayan Uplift described here comprise three members, i.e. the Karagas Group, the Oselok Group, and the Moty Group (Fig. 8). Both the Karagas and the Oselok Groups are ~3 km sedimentary successions, and both are subdivided into three Formations, corresponding to distinct fluvial cycles (Sovetov et al., 2007). The Karagas Group consists of three formations, including the Shangulezh, the Tagul and the Ipsit formations. The Ar-Ar dating results of high Mg-tholeiitic sills that form a part of the Irkutsk large igneous province (Ernst et al., 2016) allow to constrain sedimentation age of the Karagas Group between 740 and 612 Ma for upper part of the Karagas Group (Gladkochub et al., 2006), consistent with $\delta^{13}C$ evidence for pre-Ediacaran (ca. 650 Ma) time sedimentation (Sovetov and Komlev, 2005). However, an alternative U-Pb baddeleyite age of 1641 ± 8 Ma reported by Metelkin et al. (2011) for the Nersa Complex may indicate a much older age of the Karagas Group sedimentary rocks, although the study does not provide details on field relationship of the rock and dating results. This result requires that the lower part of the Karagas Group is coeval with the Mesoproterozoic deposits of the Urik-Iya graben, but such an estimate contradicts the geological relationship. The Oselok Group unconformably overlies the Karagas Group. Similarly, it consists of three formations including the Marnya (400–660 m), the Uda (200–550 m), and the Aisa (1500 m) (Sovetov et al., 2007). The Moty Formation of fluvial red cross-bedded sandstone unconformably overlies the Oselok Group, as evidenced by embedding of a ~3 m thick conglomerate layer into its bottom. Several lines of evidence indicate that the deposition of the Oselok Group and the Moty Group occurred during the late Ediacaran (Letnikova et al., 2013) and the Early Cambrian (Kochnev and Karlova, 2010), respectively. Upward the stratigraphic succession a major shift in lithology occurs, marking transition from fluvial to shallow-marine platform deposition.

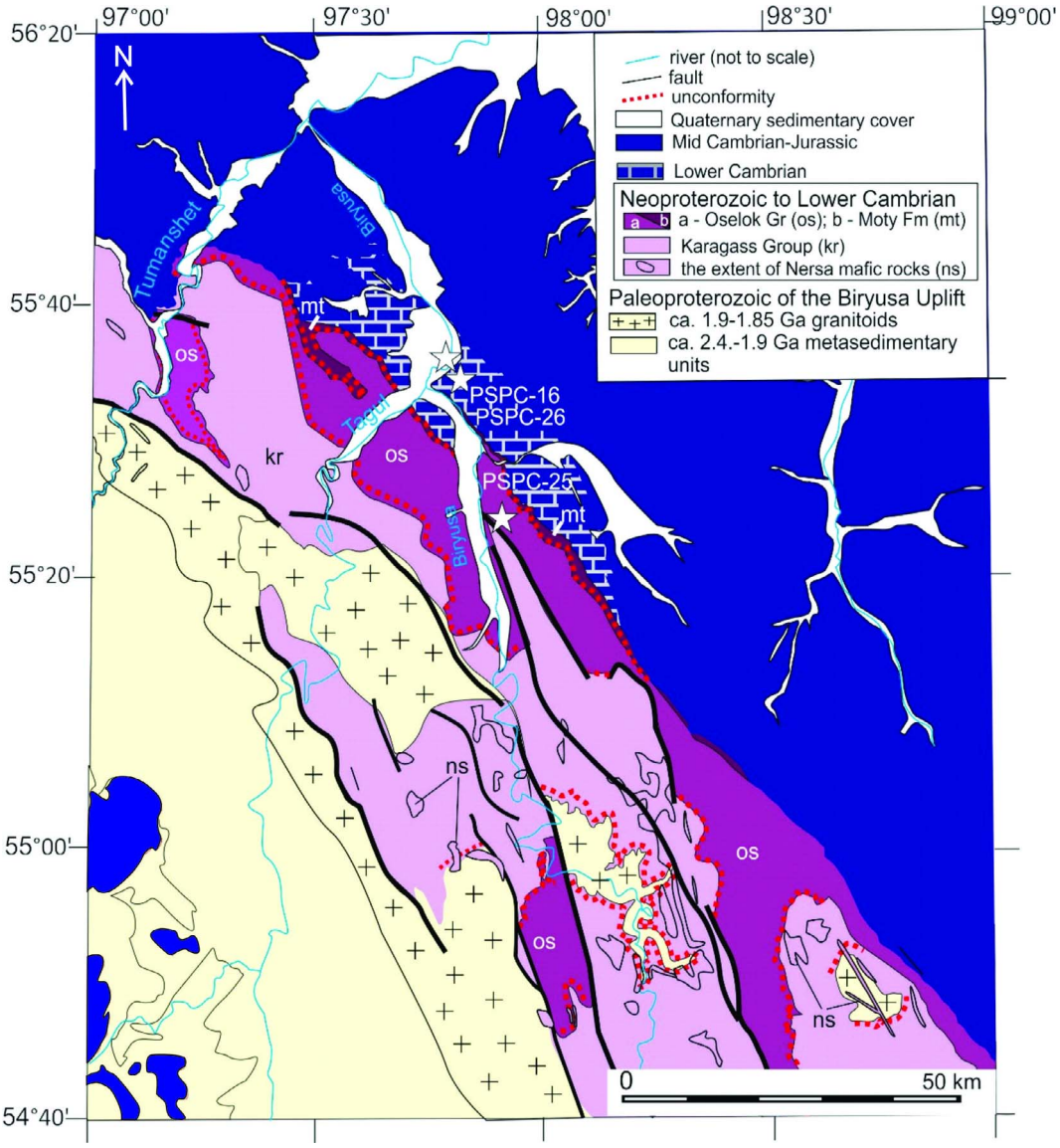

Fig. 7. Geological map of the study area in the Biryusa-Prisayan Uplift, simplified after Galimova et al. (2012), Komarevsky and Zhukov (1964), Sukhanova (1957).

4.2. Description of sampled rock units

The Shangulezh Formation, also referred to as the lower Karagas, is dominated by alluvial facies deposits including conglomerates, gravelites and coarse grained red sandstone, replaced with dolostone in the upper part of the Formation (Shenfil', 1991). Facies transition of alluvial siliciclastics to dolomites in the upper part of the Formation suggests that a sea transgression occurred in an evolving rift basin during the deposition of the Shangulezh Formation (Sovetov et al., 2007). The Shangulezh sandstones are represented by high-alkali quartz arenites and arkoses (e.g., Motova et al., 2013). The studied sample PSPC-12 is a coarse grained subarkosic litharenite, which framework is poorly sorted and consists of both rock and grain fragments. Among them monocrystalline angular detrital quartz (40%), quartzite fragments (30%), plagioclase and microcline (10%), squished siltstone fragments (20%) have been observed. Both the Tagul and the Ipsit Formations comprise siliciclastic deposits including shale, siltstone, wavy- and cross-bedded sandstone, and stromatolitic and microphytolitic dolomite formed in shelf environments (e.g., Sovetov et al., 2007; Melnikov et al., 2005; Metelkin et al., 2010). The samples PSPC-2 and PSPC-3 are subarkosic lithic wackes. Their frameworks (up to 80% of total thin section area) are poorly sorted, consist of monocrystalline angular detrital quartz (40–60%), feldspar including plagioclase and microcline (10%), rock fragments represented by quartzite (10–30%) and squashy siltstone (20%). The cement constitutes up to 20% of total thin section area and has calcareous composition. Sedimentary structures of the upper Karagas sandstones were accumulated in the shallow marine environments near storm wave-base and in the lagoonal settings (Metelkin et al., 2010).

The Oselok Group is separated from the Karagas Group by an unconformity and conglomerate horizon (Galimova et al., 2012; Letnikova et al., 2013; Sovetov et al., 2007; Sukhanova, 1957; Shenfil', 1991). The lower Marnya Formation incorporates glaciofluvial, fluvial and shallow marine facies, whereas deposition of the upper Uda and the Aisa Formations was linked to deltaic environments (Sovetov et al., 2007; Sovetov and Komlev, 2005). Grey-coloured sandstones of the Oselok Group exhibit trough and planar cross-bedding with the latter indicating an eastward direction of paleocurrent, and abundant ripple marks (Fig. 8c).

The Oselok Group is dominated by quartz-rich arkoses, lithic arenites, pelitic rocks (Letnikova et al., 2013; Motova et al., 2016). The studied samples PSPC-8 and PSPC-25 belong to the Uda and the Aisa Formations, respectively (Galimova and Pashkova, 2012), and are represented by lithic arenites. They preserve subangular, poorly sorted,

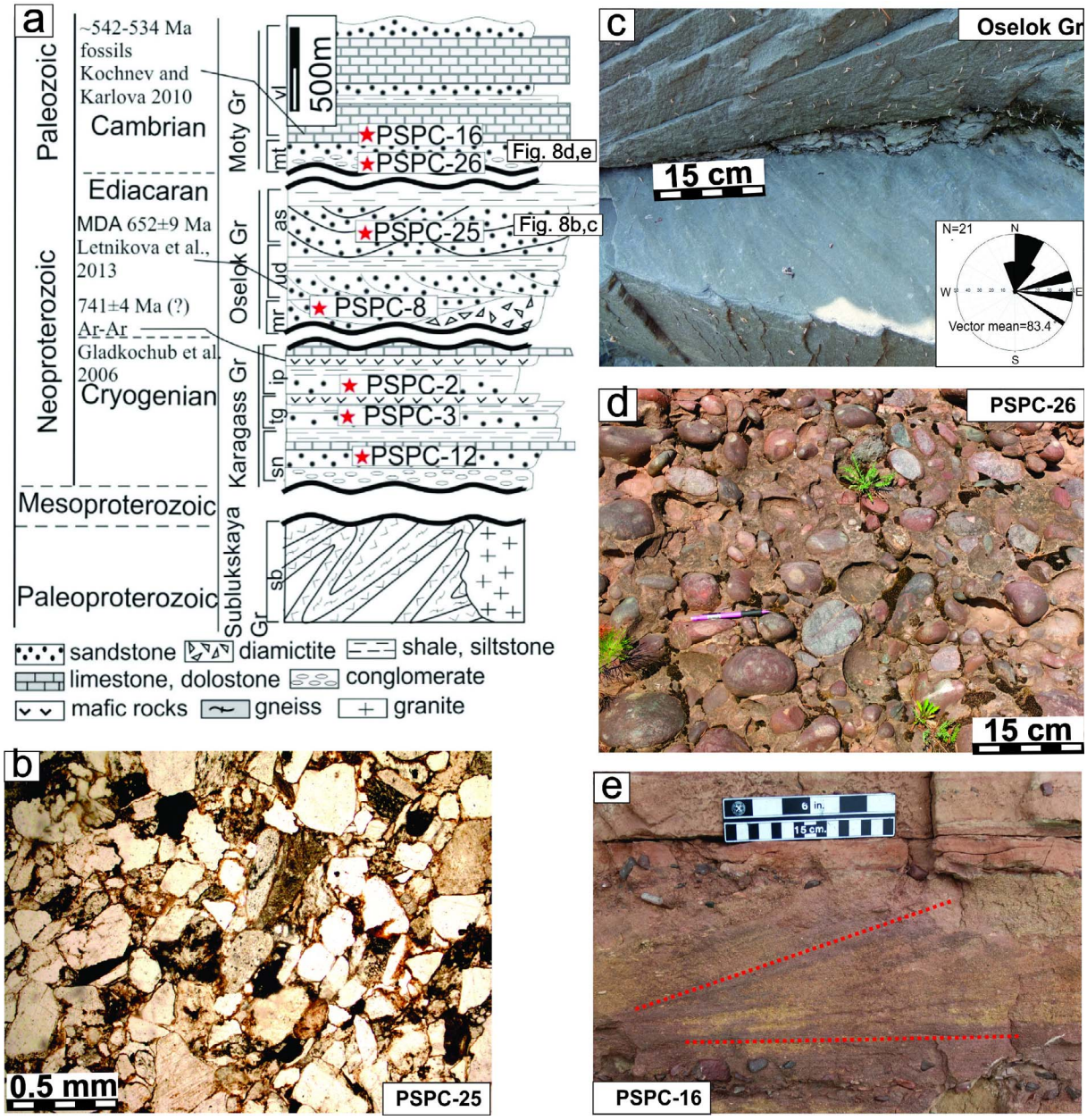

Fig. 8. Schematic stratigraphy of the Neoproterozoic and Cambrian rocks from the Prisayan Uplift and underlying metasedimentary units (a), simplified after Rasskazchikov (1958), Sukhanova (1957), Kalinovsky and Smolyanets (1965), Komarevsky and Zhukov (1964); (b) shows microphotograph of the immature sandstone PSPC-25 from the Oselok Group, parallel light; (c) fluvial sandstone of the Oselok Group with cross bedding and ripple marks and overall measured cross bedding orientation (inset) indicating general northeastern direction of paleocurrent (combined for both the Oselok and the Moty Group); and (d) shows fragment of its ~3 m thick basal conglomeratarte layer; (e) shows red fluvial sandstone and embedded pebbles of the Moty Formation. Symbols on (a): sb = Sublukskaya Formation; sn = Shangulezh Formation; tg = Tagul Formation; ip = Ipsit Formation; mr = Marnya Formation; ud = Uda Formation; as = Aisa Formation; mt = Moty Formation; vl = Verkholenka Formation. (For interpretation of the references to colour in this figure legend, the reader is referred to the web version of this article.)

both grain and rock fragments, of which ~40% are represented by monocrystalline and polycrystalline quartz, and another ~40% are deformed fragments of siltstone and phyllite. These microscopic observations suggest formation of rocks via recycling of igneous, metamorphic and sedimentary provenance. The abundance of chlorite, muscovite, serpentine, as well prismatic amphibole (~5%) is consistent with geochemical and field evidence for mixing between mafic and mature clastic components of the rocks (Letnikova et al., 2013; Motova et al., 2016). Apatite, zircon and green tourmaline are specific accessory constituents of the Oselok sandstones (5%).

The Moty Formation consists of fluvial red crossed beds, whose thickness does not exceed 150 m. Similar to coeval sandstones of the Redkoles Formation in the Yenisey Ridge, the studied sandstones PSPC-16 and PSPC-26 are represented by a medium-grained lithic arenite. The rocks consist of a poorly sorted framework (~95%) dominated by subangular grain and sedimentary rock fragments, and the limonite-rich cement, which makes up to 5% of the rock. The main components of the framework include monocrystalline quartz (~50%), polycrystalline quartz (~10%), detrital magnetite (~10%), feldspars (< 5%) and siltstone fragments (~30%). Rare garnet, zircon and secondary muscovite occur as accessory phases.

4.3. Results of U-Pb and Lu-Hf analysis

Three samples PSPC-12, PSPC-2 and PSPC-3 characterise sedimentary rocks of the Karagas Group. The sample PSPC-12 had 110 grains

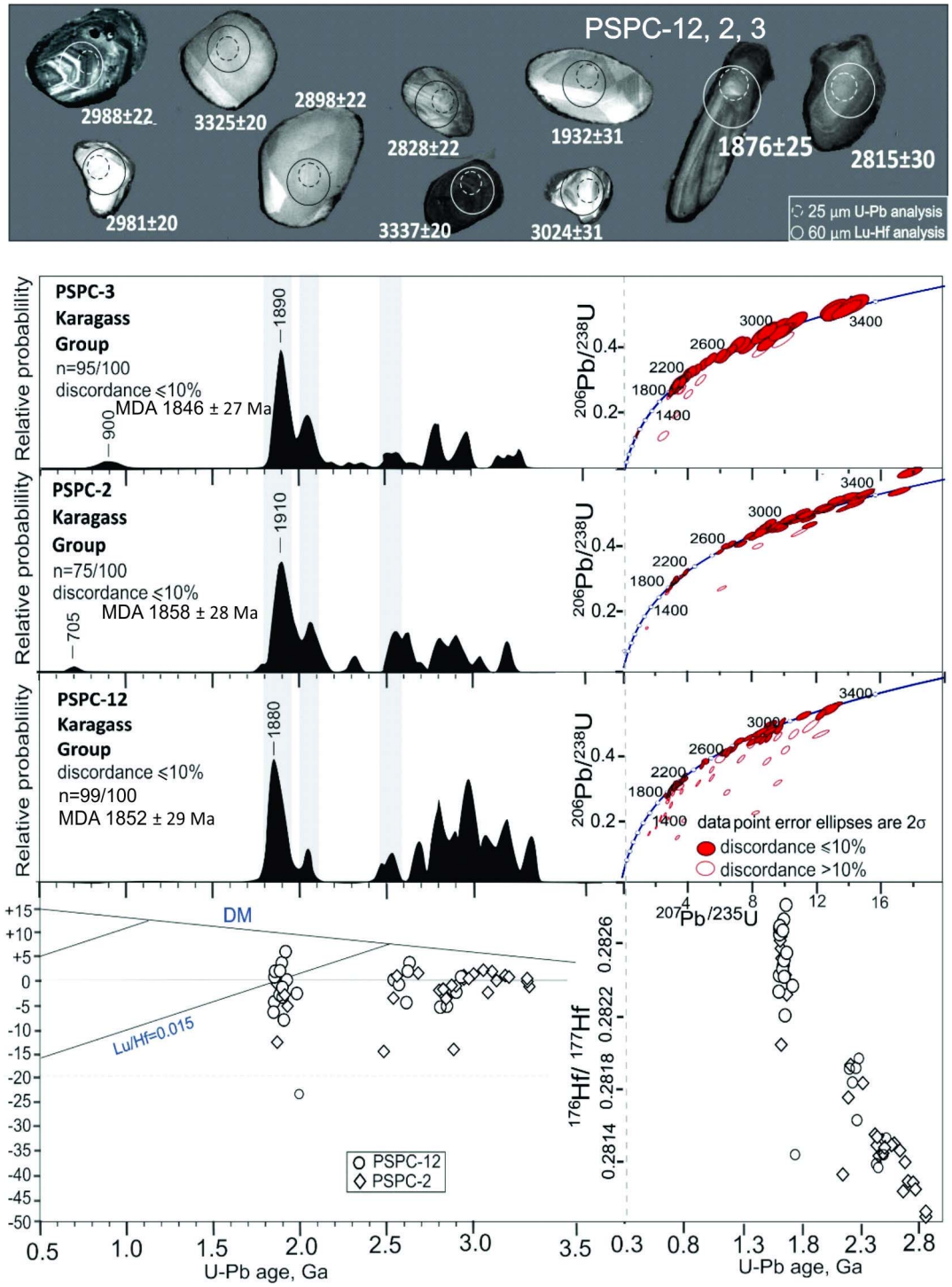

Fig. 9. Age spectra, concordia plots, εHf (T) versus age and $^{177}Hf/^{176}Hf$ ratio versus age of detrital zircon populations for the Karagas Group, supported by CL images of selected grains.

analysed (Supplementary file 2), of which 99 met the 10% discordance criteria (99/100); 75/100 and 95/100 age determinations from the samples PSPC-2 and PSPC-3 were suitable for further interpretation, respectively. The majority of filtered analysis plot on the concordia, excluding few data points that plot near concordia (Fig. 9). Detrital zircons recovered from the three samples yield conformal age spectra (Fig. 9). Each of the spectra incorporates three main age clusters of ~1970–1820 Ma, ~2120–2100 Ma, 3300–2500 Ma. Prominent peaks occur at 1900–1800 Ma and 2070 Ma. The MDAs (based on the mean age of the youngest cluster) of the samples PSPC-12, PSPC-2 and PSPC-3 are 1846 ± 27 Ma (n = 3, MSWD = 0.71), 1858 ± 28 Ma (n = 3, MSWD = 0.014) and 1852 ± 29 Ma (n = 3, MSWD = 0.014). However, the presence of Neoproterozoic grains including 678 ± 11 Ma, 831 ± 30 Ma, 880 ± 32 Ma and 927 ± 33 Ma in the samples PSPC-2 and PSPC-3 from the upper part of the Karagas Group, allows to suggest its Neoproterozoic MDA. The entire zircon population exhibits rounded to subrounded morphology, typical of Archean and Paleoproterozoic grains, respectively.

In the samples PSPC-12 and PSPC-2, the majority of ca. 1970–1820 Ma age range are characterised by εHf (T) values in range between −5 to +5. Similarly, Archean grains yield εHf (T) values hovering near CHUR proxy (Fig. 9).

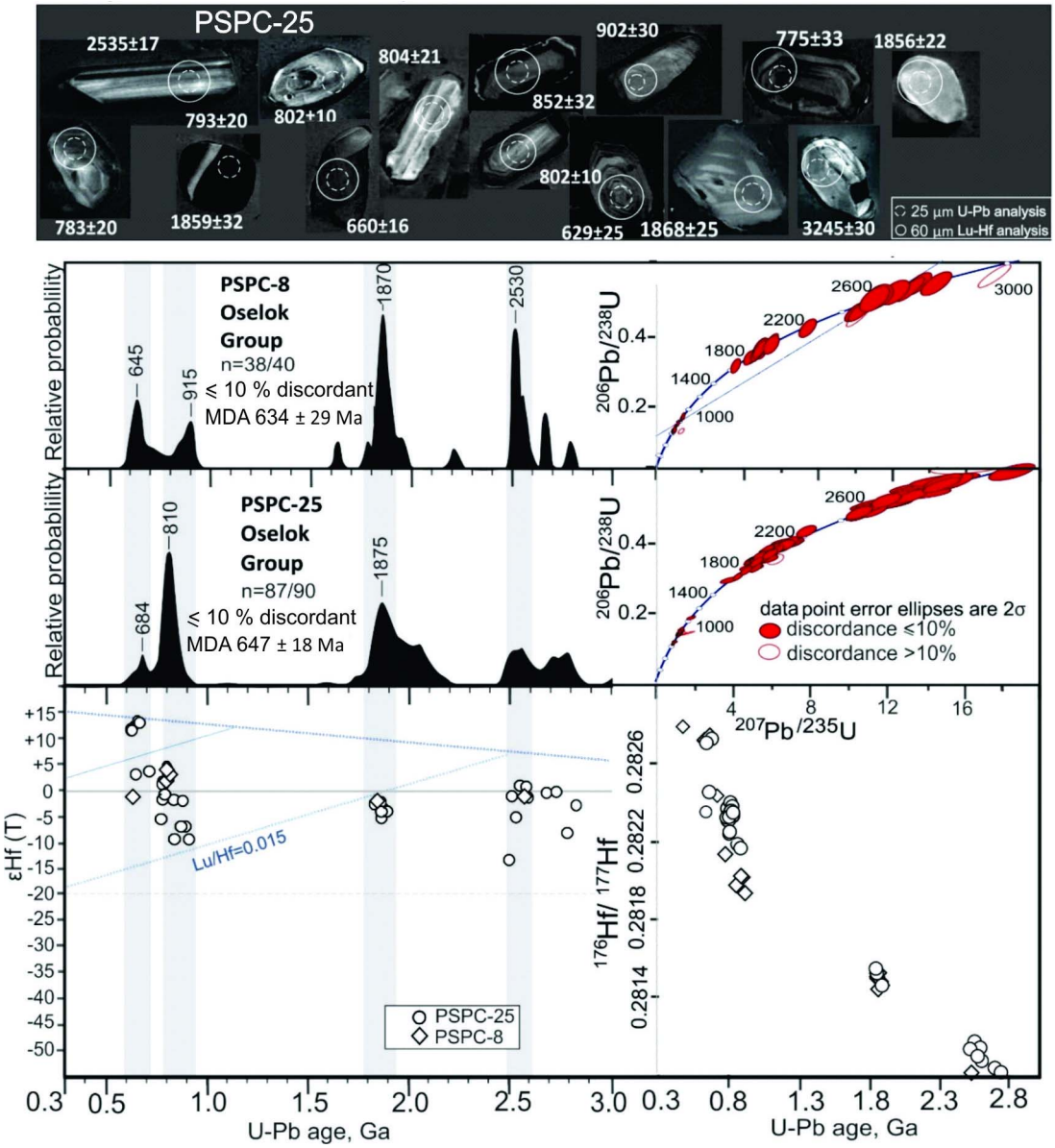

Fig. 10. Age spectra, concordia plots, εHf (T) versus age and $^{177}Hf/^{176}Hf$ ratio versus age of detrital zircon populations for the Oselok Group, supported by CL images of selected grains.

Samples PSPC-8 and PSPC-25 represent sandstones of the Oselok Group. The sample PSPC-8 yielded 40 single grain analysis (Supplementary file 2), of which 38 met the 10% discordance criteria (38/40); 87/90 suitable results were obtained from the sample PSPC-25. The samples yield Archean (~30%), Paleoproterozoic (~40%) and Neoproterozoic (~30%) zircon populations (Fig. 10), consistent with results of Letnikova et al. (2013). The Paleoproterozoic age group of zircons incorporates the major 1900–1820 Ma population with a prominent probability density peak at 1860 Ma, and the minor 2100–1900 Ma zircon population. The Archean age group of zircons incorporates (1) the Neoarchean subgroup yielding probability density peak at 2540 Ma and (2) the Paleoarchean subgroup of zircons with ages in range of 3250–3350 Ma. Both the Archean and Paleoproterozoic grains are commonly subrounded. The Neoproterozoic zircon grains are commonly euhedral, suggesting their derivation from a proximal source. They are represented by two zircon populations, including the 920–760 Ma that defines major peak at 805 Ma, and the 720–600 Ma population with a peak at 647 Ma. The MDA estimates based on the age of the youngest cluster are 634 ± 29 Ma (n = 3, MSWD = 0.0.013) for the sample PSPC-8 and 647 ± 18 Ma for the sample PSPC-25 (n = 3; MSWD = 0.61), consistent with the pre-existing constraints (Section 4.1).

In the Oselok Group sandstones, the Neoproterozoic (920–760 Ma) zircons have εHf (T) values (Fig. 10) falling in ranges between 0 and −10 at ca. 920–850 Ma, and between −5 and +5 at ca. 850–780 Ma. The 1900–1820 Ma zircon population is characterised by εHf (T) values that form a tight cluster at 0 to −5. The Archean grains have εHf (T) values hovering around and below the CHUR proxy.

Samples PSPC-26 and PSPC-16 represent sandstones from lower part of the Moty Formation. The sample PSPC-26 had 70 grains analysed (Supplementary file 2), of which 64 met the 10% discordance criteria (64/70); 71/90 suitable results were obtained out of the sample PSPC-16. Broadly, zircons from the two samples yield similar detrital age spectra (Fig. 11), with predominant Paleoproterozoic (62–71%) and Archean (15–25%) populations and subordinate Neoproterozoic (8–13%) zircon population. In both samples, Archean and Paleoproterozoic grains tend to be subrounded, although a few have been noticed to preserve facets whereas among the Neoproterozoic grains prismatic shapes prevail, although subrounded grains occur as well (Fig. 11). The Archean part of the age spectra is featured by a nearly

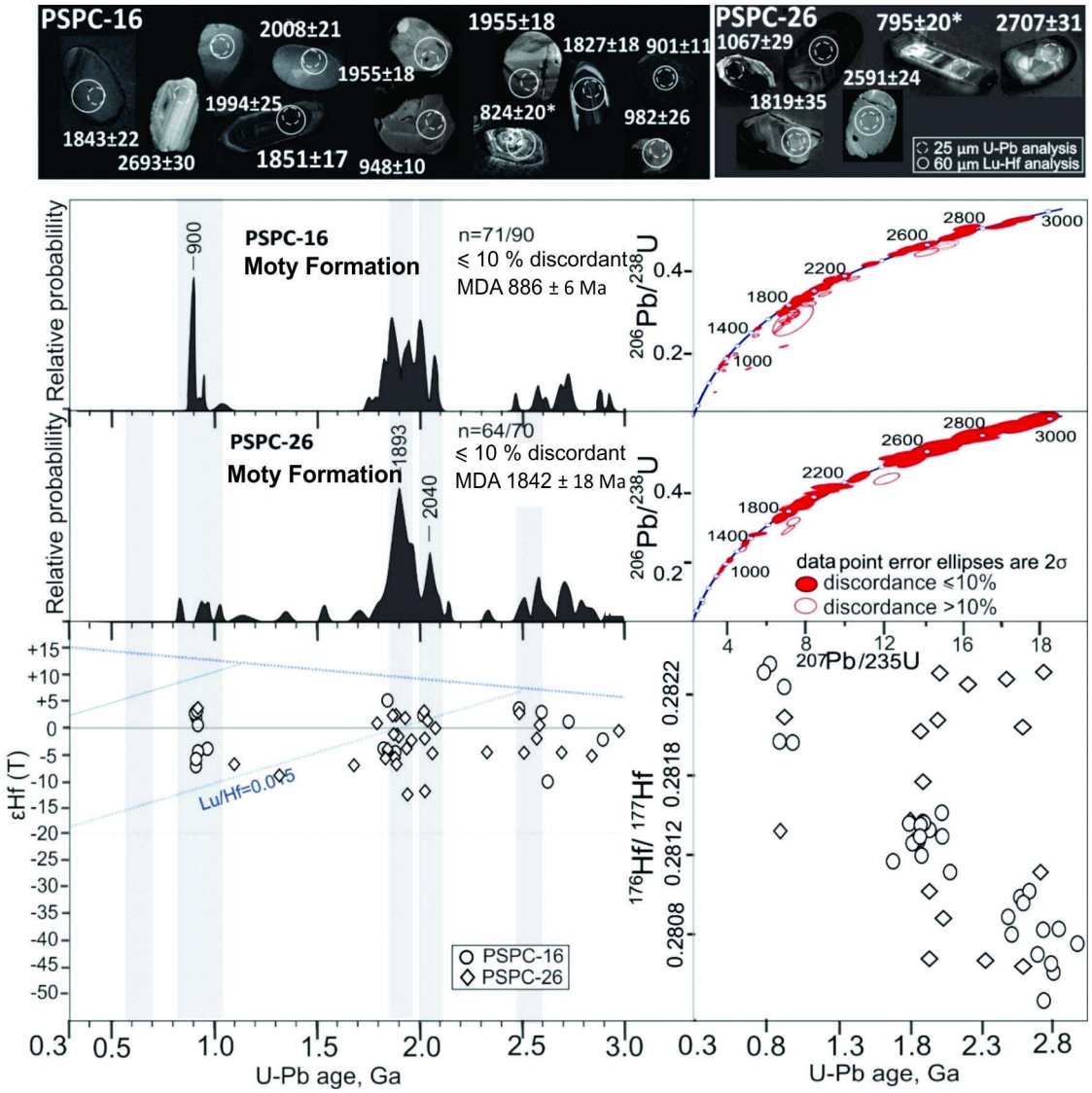

Fig. 11. Age spectra, concordia plots, εHf (T) versus age and $^{177}Hf/^{176}Hf$ ratio versus age of detrital zircons from the Moty Formation, supported by CL images of selected grains.

continuous 3000–2500 Ma signature, with no prominent peaks. Paleoproterozoic zircon ages fall within the 2100–1800 Ma interval, defining two probability peaks at 1890 Ma and at 2040 Ma, separated by probability density low at 1900 Ma. Also, a few Paleoproterozoic grains with ages of ca. 2200 Ma, ca. 2300 Ma, ca. 2460 Ma have been identified. The Neoproterozoic zircon population is only significant in sample PSPC-16, where 15% of the total grain ages fall in range between 960 and 860 Ma, with maximum probability density at 900 Ma. For the sample PSPC-16 the MDA based on the youngest zircon cluster is 886 ± 6 (n = 3, MSWD = 0.38) and for the sample PSPC-26 is 1842 ± 18 (n = 3, MSWD = 0.17). These MDAs are significantly older than Cambrian age of sedimentation inferred from other geological records (Section 4.1).

The 1000–850 Ma zircon population is characterised by εHf (T) values falling in a range between −7 to +5 and forms a strong vertical array on the εHf (T) vs. age plot (Fig. 11e). The 1950–1800 Ma Paleoproterozoic zircon population with a peak near 1870 Ma is characterised by εHf (T) values in range of +5 to −7. The majority of εHf (T) values measured for the older Paleoproterozoic and Neoarchean zircons cluster between +4 and −5 so that the age vs εHf (T) data points plot near CHUR proxy.

5. The Neoproterozoic sedimentary rock associations of the Yenisey Ridge and the Prisayan Uplift

Evolution of sedimentary basins in the Yenisey Ridge and the Prisayan areas was largely controlled by tectonic events that occurred along the western margin of the SC. In both the south Yenisey Ridge and the Prisayan regions, the Meso- to Neoproterozoic siliciclastic deposits form two main sedimentary cycles that are separated from each other by late Ediacaran angular unconformity (Fig. 12).

5.1. *Pre-accretionary rock associations*

In the Yenisey Ridge, the pre-unconformity units are represented by the Mesoproterozoic Sukhopit Group (Fig. 12a). Its sandstone and shale, overlain by shelf-type carbonate rock associations of the Neoproterozoic Tungusik Group, may be correlated (Priyatkina et al., 2016, and ref. therein) to the Kamenskaya Group of the Turukhansk Uplift (Petrov, 2006). Similar to the Karagas Group, metasedimentary units of the Sukhopit Group overlie the basement units of the Paleoproterozoic Angara Fold Belt (Fig. 1) and bears its erosional products (Priyatkina et al., 2016).

In the Prisayan area, deposits of first sedimentary cycle are represented by the Karagas Group. The minimum age of syndepositional

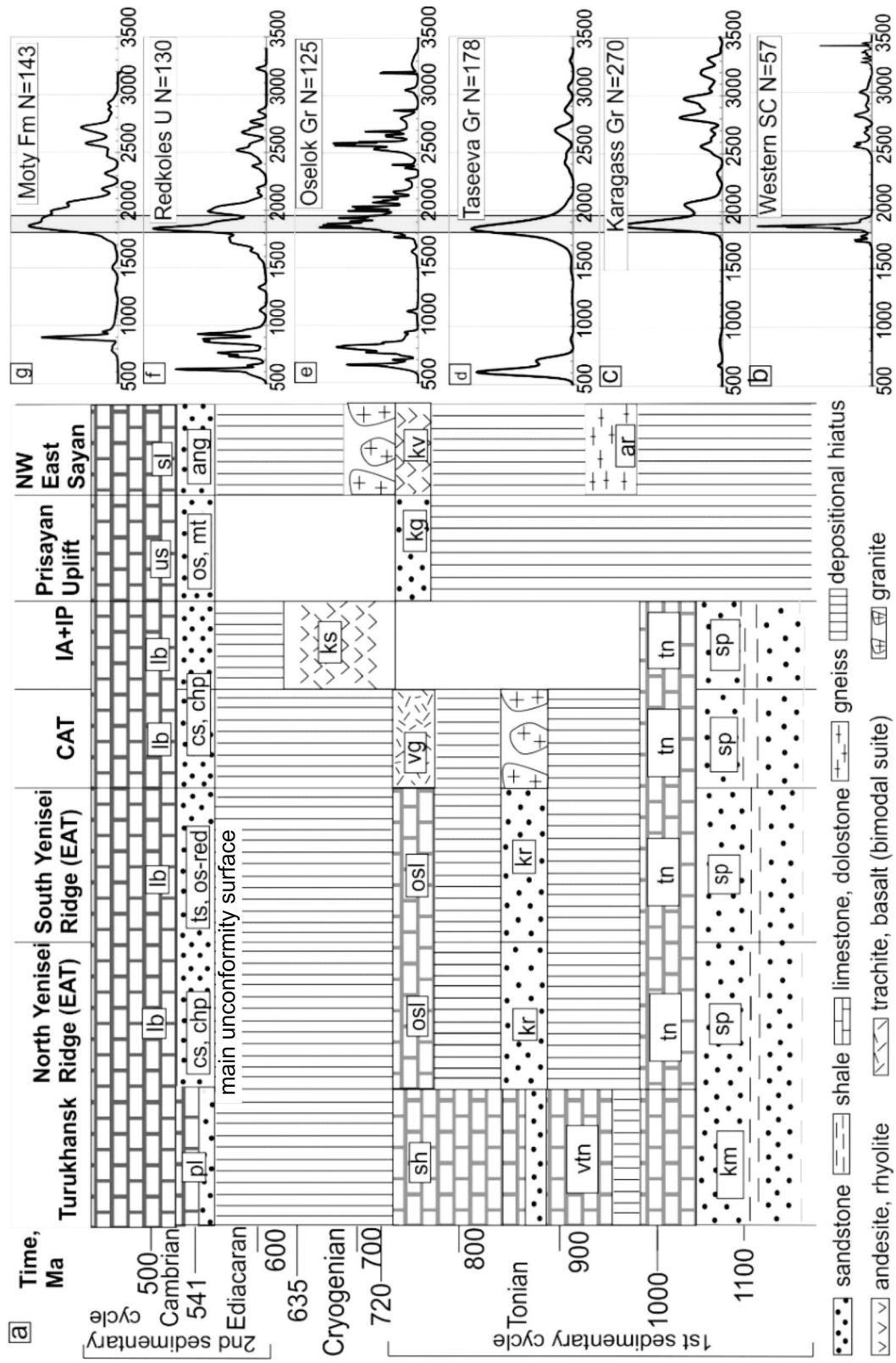

Fig. 12. Comparative chart (a) showing the evolution of late Mesoproterozoic and Neoproterozoic sedimentary basins along the western margin of the SC (Siberian Craton). Source data for magmatism are in Supplementary file 3; sedimentary records compiled using Postnikov et al. (2008), Petrov (2006), Sovetov et al. (2007), Vernikovsky et al. (2009), geological maps of Russia in scale 1: 1,000,000, including (Bezzubtsev et al., 2008b; Galimova and Pashkova, 2012; Kachevsky and Zuev, 2009; Varganov et al., 2010), and a comparison between total U–Pb detrital zircon age spectra between the early Precambrian basement (b), the Neoproterozoic (c–e) to Early Cambrian sedimentary rocks (f, g) of western Siberian cratonic margin. Source data and references for (b) are given in Supplementary file 3. Symbols: km – Kamenskaya Group, sp – Sukhopit Formation, vtn – Verknetungusik group, tn – Tungusik Group, kr – Krasnogor Formation, osl- Oslyanka Group, ar – Arzibei Group, kg – Karagas Group, kv – Kuvai Group, ks- Kutukass Group, pl – Platonovskaya Formation, cs – Chingasan Group, chp – Chapa Group, ts – Taseeva Group, os-red – Redkoles Formation, mt – Moty Formation, lb – Lebyazhinskaya Formation, us – Usol Formation, sl – Solb'a Formation.

Nersa sills and other records such as stromatolites, microphytollites, isotope geochemistry suggest that the deposition of the Karagas Group could have occurred near ~740 Ma (Gladkochub et al., 2006; Stanevich et al., 2007), consistent with presence of Neoproterozoic grains in samples PSPC-2 and PSPC-3 (Fig. 9). The presence of a zircon grain as young as 687 ± 11 Ma in the sample PSPC-2 reinforces the possibility of Ediacaran age for the upper parts of Karagas (Gladkochub et al., 2006; Sovetov and Komlev, 2005). However, an older age for the lower part of Karagass succession is possible.

Detrital zircon age analysis indicate that the Karagas Group formed at the expense of 2100–1800 Ma and 3400–2500 Ma suites (Fig. 12b), which are widespread in the Sharyzhalgai and Biryusa uplifts (e.g., Donskaya et al., 2014; Poller et al., 2004; Turkina et al., 2006, 2013; see Fig. 12c for probability age distribution plot and Fig. 1 for location). Significant thickness of up to ~4 km of dominantly siliciclastic lithologies, and large gap between cluster-based MDAs and the sedimentation age favours a divergent setting of the Karagas Group, which could allow for contribution of clastic material from Archean and Paleoproterozoic crust of south-western SC. One option is that such setting was the Siberian passive margin (Metelkin et al., 2010; Pisarevsky and Natapov, 2003; Sklyarov et al., 2002). However, relatively immature lithologies (Sections 4.2 and 4.3) and chemical composition of embedded sills (Gladkochub et al., 2006) also permit deposition of the Karagas Group in a rift setting or along a rifted margin proximal to an extending back-arc basin.

5.2. Post-accretionary rock associations

In the study areas, the surface of major angular unconformity is directly overlain by fluvial successions of Taseeva, Oselok, Redkoles, Moty (Fig. 12a). Their late Ediacaran to earliest Cambrian age has been previously constrained by fossil records and is consistent with cluster-based MDAs (Sections 3.1,3.3 and 4.3), broadly consistent with deposition in a convergent plate margin setting.

The studied post-unconformity sedimentary units of the Yenisey Ridge formed at the expense of ca. 2700–2500 Ma, 2000–1750 Ma and 950–650 Ma metasedimentary and igneous detrital fragments (Sections 3.2, Figs. 5, 6, 9, 10 and 12d, f), consistent with erosion of pre-unconformity rock associations of the CAT, IPT and AKT such as the Sukhopit Group (e.g., Priyatkina et al., 2016), granites of Teya-Yeruda, Ayakhta-Chirimba, Tis, Garevka, Glushikha, Ostyatski, Vorogovka, Tatarka-Ayakhta, Predivinsk (Likhanov et al., 2011, 2012, 2013, 2014; Likhanov and Reverdatto, 2014a; Kozlov et al., 2012; Kuzmichev and Sklyarov, 2016; Nozhkin et al., 1999, 2008, 2011, 2013, 2015a,b; Vernikovskaya et al., 2002, 2003, 2007; Vernikovsky et al., 2003, 2007, see Supplementary file 3) into the hypothetical Taseeva foredeep basin. Immature character of the samples (Fig. 4b, c), results of detrital zircon analysis, paleocurrent analysis of Sovetov and Blagovidov (2004) indicating main eastward transport direction for the sediments, are all consistent with this interpretation. Broadly similar to the post-unconformity sedimentary rocks of the Taseeva basin, the studied post-unconformity sedimentary units of the Prisayan Uplift formed at the expense of ca. 3000–2500 Ma, 2200–800 Ma and 950–650 Ma suites (Figs. 5, 6, 9, 10 and 12e, g). Contribution of clastic material derived from Neoproterozoic igneous suites was significant, in agreement with lithogeochemical and detrital zircon study of Letnikova et al. (2013), Motova et al. (2016) and also consistent with ages of rock associations, which are widespread in the north-western East Sayan, such as the granitoids of the Arzibei, Kan, Shumikha-Kirel, and Kuvai calc-alkaline volcanic rock associations of the Derba terrane (e.g., Bezzubtsev et al., 2008b; Nozhkin et al., 2001; Turkina et al., 2004, see Supplementary file 3). Nonetheless, Neoproterozoic terranes were not the only provenance for these rocks. Lithic arenites, wackes and arkoses of the Oselok and the Moty Group groups contain ca. 3.3–2.5 Ga and ca. 2.2–1.8 Ga detrital material characteristic of the underlying pre-unconformity successions such as the Karagas Group (compare Fig. 12c, e, g). One option is that both pre- and post-unconformity sediments received their detritus from proximal Archean and Paleoproterozoic crustal units of the SC. Alternatively, in our preferred interpretation, the post-unconformity units could have formed through cannibalisation of the underlying metasedimentary basement and therefore both have similar detrital signatures. Same as in the Yenisei Ridge area, lithic clasts from the pre-unconformity units of the Prisayan Uplift constitute up to 40% of the framework in sandstones of the post-unconformity Oselok and Moty groups.

The Oselok Group could have accumulated along the Siberian passive margin as previously suggested by Letnikova et al. (2013) and Pisarevsky and Natapov (2003), who point out an increase in thickness from the northeast to southwest. In this case, the abundant Neoproterozoic detritus could have been supplied from the Neoproterozoic suites of the Yenisey Ridge, broadly coeval to those of the north-western Sayan. However, Archean and Paleoproterozoic detrital signatures in the Yenisey Ridge area and the Prisayan Uplift are not identical, suggesting that these sedimentary basins were isolated from each other. Also, neither the presence of bimodal volcanic rock association as fragments within rock framework, nor the evidence for immature rock character such as the presence of feldspars, heterogeneous rock fragments, and their variable rounding (Letnikova et al., 2013; Motova et al., 2016, this study) are consistent with a passive margin setting. Furthermore, sedimentary textures such as cross-bedding (Fig. 4c, e) indicate a shallow depositional environment. Although our dataset for the Oselok and Moty groups is too small to draw solid conclusions, the preliminary results of paleocurrent analysis indicate general northeastward paleocurrent direction. Thus for both Oselok and Moty groups foreland setting allowing for erosion of proximal sedimentary, magmatic and metamorphic suits appears to be more probable. A rift setting (e.g., Sovetov et al., 2007), proximal to orogenic suites could be also permissive, although there is no evidence for any contemporaneous rift-related magmatism in this sedimentary basin.

6. Hf isotopic evolution of the western SC margin

In this paper we aim to identify cratonic affinity of the Neoproterozoic crust presently located along the western SC margin by comparing detrital zircon populations established on the western margin of the SC below and above the main Ediacaran unconformity surface, and by also discussing the geological evidence and Hf in zircon data.

6.1. Hf isotopic evolution of the western SC margin

The early Precambrian crust of western SC, viz. the Angara belt, comprises 2.0–1.75 Ga and possibly older 2.1 Ga magmatic and metamorphic suites, as well as 3.4–2.5 Ga tonalite-trondjemite rock associations, granulites and plagiogranites (Supplementary file 3). Their εHf (T) values including those recalculated from εNd (T) using the equation 1.36εNd + 2.95 of Vervoort and Blichert-Toft (1999) are presented in Fig. 13a and in Supplementary file 3. In εHf (T) vs age space, the compositions of Archean zircons plot parallel to CHUR, with the majority of εHf (T) clustering between −5 and +7. Igneous rocks with ages in the range 2000–1900 Ma are characterised by dominantly positive εHf (T) in range between −1 to +6, whereas igneous rocks with ages in range 1800–1700 Ma have negative εHf (T) of 0 to −7. εHf (T) values of the major 1900–1850 Ma zircon population range from −12 to +3, forming an extended vertical array, suggesting that the host magma was derived from partial melting of multiple sources. In contrast to many other cratons, the Precambrian basement of the SC lacks Mesoproterozoic orogenic belts (Rosen et al., 1994; Glebovitsky et al., 2008; Rosen and Turkina, 2007). This phenomenon was also identified by Gladkochub et al. (2010a) with particular reference to the southern SC.

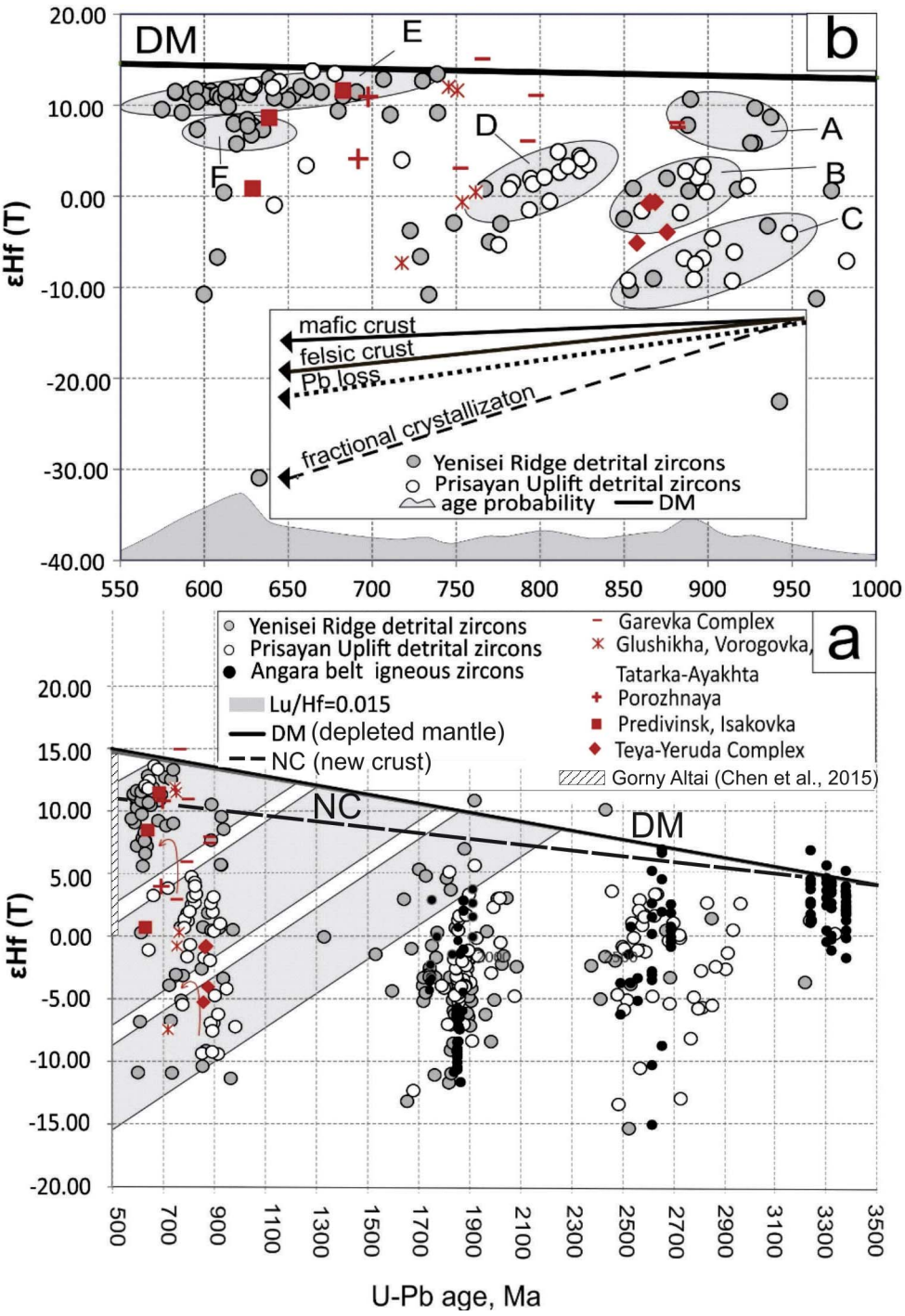

Fig. 13. Hf isotope compositions vs. U–Pb age plot for detrital zircons recovered from Neoproterozoic to Lower Cambrian sedimentary rocks of western Siberian cratonic margin, compared with an isotopic signature of the Angara belt (a). Inset (b) is enlarged plot of Neoproterozoic data points. Original and published source data are presented in Supplementary file 2. The isotope evolution of mafic crust is based on $^{176}Lu/^{177}Hf = 0.022$ (Blichert-Toft and Albarède, 2008), the evolution of upper felsic continental crust based on $^{176}Lu/^{177}Hf = 0.008$ (Rudnick and Gao, 2003), mafic crust are shown for reference, assuming silicate Earth differentiation at ~4.5 Ga (Bennett et al., 2007). The dashed line is fractional crystallization (Spencer et al., 2015).

6.2. Sources of Neoproterozoic magmatic systems

The studied syn- and post-orogenic Neoproterozoic to Lower Cambrian rocks from western SC margin were derived from proximal sources, as evidenced from the occasional presence of igneous rock fragments and immature textures of rock samples (Sections 3.2 and 4.2). The zircons are characterised by Th/U ratios of > 0.07 (Supplementary File 2), suggesting igneous origin (e.g., Hoskin and Schaltegger, 2003). The majority of zircon grains also exhibit igneous textures. Thus, the samples can be used to characterise main magmatic belts of the Yenisey Ridge and the north-western East Sayan Mountains.

The Neoproterozoic part of the integral detrital zircon age spectra (Fig. 13b) contains 1000–750 Ma and 750–550 Ma intervals separated by a density low at ~750 Ma, further referred to as early and late Neoproterozoic peaks. The former can be further subdivided into the 950–830 Ma and 830–750 Ma age groups, separated by a low.

Provided that the sources of clastic material were local, the early Neoproterozoic zircon populations can only be linked with the S- and I-type granites of the Yenisey Ridge and the north-western Prisayan. The 830–750 Ma age cluster is associated with granitoids often referred to as transitional between the S- and A-types (Kozlov et al., 2012) such as the Garevka massif (Likhanov and Reverdatto, 2015; Vernikovskaya et al., 2006; Vernikovsky et al., 2003), typical A-type granites exemplified by the Chirimba, Ayakhta, Strelkovsky, Glushikha granites (Vernikovskaya et al., 2003, 2002, 2007; Vernikovsky et al., 2007), A-type granites and bimodal volcanic suites of the Vorogovka trough

(Nozhkin et al., 2011, 2013, 2008), metamorphic rocks of the Angara-Kan massif (Nozhkin et al., 2016) and possibly the Kuvai Group of north-western Prisayan (Bezzubtsev et al., 2008b).

The isotopic information about sources of the Neoproterozoic magmatic suites that occur along the present western SC margin was previously limited to a Nd array with ~εNd (T) values that range between −10 and +8 (Turkina et al., 2007) as well as individual data points equivalent to εHf (T) values that range between −7.5 to +12.5 (see Supplementary file 3). Implication of these datasets for understanding the crustal growth in the western SC is important, but their interpretation in terms of magmatic and tectonic history of the area is complicated by (1) usage of sedimentary rocks to obtain meaningful Nd model ages, (2) phenomena of magma mixing (Goldstein, 1987) and (3) uncertainty of primary isotopic ratios in the protolith rocks. Issues (2) and (3) are also critical in interpretation of Hf in zircon isotopic data (Payne et al., 2016) including those presented here.

Nonetheless, Hf in zircon data presented in sections 3.3 and 4.3 provide new information on the tectonic setting of these magmatic systems. Broadly, the Neoproterozoic Hf array (Fig. 13) is consistent with those of typical accretionary orogens (Collins et al., 2011). The 950–850 Ma zircon population forms a subvertical mixing array in εHf (T) space (Fig. 13a), typical of zircon populations associated with continental arcs (Griffin et al., 2002; Linnemann et al., 2014; Smits et al., 2014; Yang et al., 2007). A more detailed analysis (Fig. 13b) indicates that three main clusters of εHf (T) values define three main source contributors to the early Neoproterozoic magmatic rocks of the Yenisey Ridge and north-western East Sayan (A, B and C). (A) represents an isotopically evolved component, (B) a component equivalent to CHUR and (C) a juvenile component equivalent to mantle, juvenile crust or a reservoir of New Crust (Dhuime et al., 2011). Similar to (B), εHf (T) values of the 850–750 Ma zircon population vary between −2 and +5 (component D). The majority of 750–550 Ma zircons are characterised by positive εHf (T), defining two juvenile magma source components (E and F). Three clusters of ~εHf (T) versus age data points (B–D on Fig. 13b) yield steep regression lines comparable with those of North Atlantic Orogen (Spencer et al., 2015) and sometimes interpreted as the rate of reworking (Spencer, 2016). The axis of cluster E approximates the evolution of mafic crust with high Lu/Hf ratios (Fig. 13b). Clusters A and F form isolated clouds and do not produce apparent trends.

6.3. Cratonic affinity of the Yenisey Ridge and the north-western East Sayan magmatic systems

Several lines of evidence suggest that the ancient crustal sources, reworked during the ca. 950–850 Ma and 750–600 Ma continental arc magmatism, were in early Precambrian basement of the Siberian margin.

First of all, the pre-Neoproterozoic intervals in detrital zircon age spectra of the pre- and post-orogenic sedimentary rocks of western SC are similar (Fig. 12b–g), suggesting that there was no addition of an exotic, non-Siberian crustal material to the orogen. Furthermore, emplacement of extensive 870–820 Ma magmatic belt into the Siberian plate is supported by zircon lead loss/development of low-T mineral assemblages in the pre-unconformity metamorphic rocks and sedimentary successions of the Turukhansk, AKT, and the Sharizhalgai uplift (Gorokhov et al., 1995; Nozhkin et al., 2013; Semikhatov and Serebryakov, 1983; see Figs. 1 and 2 for location). Moreover, zircon inheritance in the Glushikha granites and Kuvai volcanic association (Bezzubtsev et al., 2008b; Nozhkin et al., 2013), and widespread metamorphism within the CAT, AKT and the Biryusa Uplift (e.g., Nozhkin et al., 2007, 2015b, 2016; Turkina et al., 2007, Fig. 2) during ca. 750–600 Ma suggest that the early Neoproterozoic magmatic belt served as the basement to younger magmatic suites of the IPT, Kuvai terrane and possibly Arzibei and Derba block (Fig. 2).

Another important link between the Siberian margin and its Neoproterozoic fringe is occurrence of several common fragments (Fig. 2). In the Yenisey Ridge, the Sukhopit and the Tungusik groups occur within the EAT, CAT, and IPT (e.g., Kachevsky and Zuev, 2009; Varganov et al., 2010), providing a framework for restoration of a Mesoproterozoic continental slope of western SC margin across the Yenisey Ridge (Khabarov and Varaksina, 2011; Postel'nikov, 1980). Furthermore, the granites equivalent to the ~2600–2500 Ma Kitoi terrane (Gladkochub et al., 2005) occur as fragments within the CAT (Kuzmichev and Sklyarov, 2016), suggesting a genetic link between the basements of the western SC and the CAT. However, pure coincidence is possible: the known occurrences of the 2600–2500 Ma crustal complexes are significant in the north-western SC (Priyatkina et al., 2016), North China (Geng et al., 2012) and Rae Craton (Bethune, 2015). Similarly, Proterozoic coexistence of sedimentary basins in the north-western Sayan and the Prisayan Uplift can be suggested. Both stratigraphic sections (Fig. 12) are characterised by paucity of Mesoproterozoic sedimentary rocks, and correlation between the upper Ediacaran – Lower Cambrian Moty, Angul', Usol, Sol'ba formations (e.g., Bezzubtsev et al., 2008a; Galimova and Pashkova, 2012; Postnikov and Terleev, 2004) of the north-western East Sayan and the Prisayan Uplift favours juxtaposition between the two terranes in the late Precambrian.

Siberian affinity of the above mentioned terranes suggests that a subduction zone existed near the western margin of the SC during the Neoproterozoic, such as shown by Metelkin et al. (2012) and Kuzmichev and Sklyarov (2016) for some intervals of the Neoproterozoic, and conflicts with paleomagnetic evidence of Vernikovsky et al. (2016), which suggests that the Neoproterozoic crust of the Yenisei Ridge was exotic to Siberia. If the Neoproterozoic terranes which are now located in the close proximity the Taseeva basin of the Yenisey Ridge and the Prisayan Uplift were exotic, an exotic in respect to the SC detrital signatures in post-accretionary sedimentary rocks would have been observed. The presence of both the Siberian (this study) and exotic to Siberia Neoproterozoic crustal fragments (e.g., Rojas-Agramonte et al., 2011) near the south-western margin of the SC reinforces the significance of major Paleozoic tectonic boundary between the north-western and the south-eastern Sayan (Fig. 2b).

7. Neoproterozoic accretionary events along the south-western margin of the SC

In the following, we discuss main evolutionary stages of the western Siberian margin (Fig.14) drawn from integration of U–Pb–Hf detrital zircon and geological records.

7.1. Phase 0 (pre-Neoproterozoic history)

The crystalline basement of the Yenisey Ridge is formed by early Precambrian granulite-gneiss and schist–gneiss complexes injected by collisional and anorogenic granitoids with an age of 1.84 and 1.75 Ga, respectively (Nozhkin, 2009). The later history of the margin involved deposition of the Sukhopit Group, which age has been roughly constrained between ~1650 Ma and ~1050 Ma (Nozhkin, 2009 and ref. therein), extension and emplacement of bimodal volcanic suites and A-type magmas (Gladkochub et al., 2002; Popov et al., 2010).The Sukhopit succession has been interpreted as passive margin fragment (Pisarevsky and Natapov, 2003; Nozhkin, 2009) but other extensional settings are also permissive (e.g., Priyatkina et al., 2016). Thus, a deeper understanding the Mesoproterozoic evolution of the western SC margin requires further investigations.

7.2. Phase 1 (950–840 Ma)

Continental arc setting near the western SC is reflected by a vertical Hf array, consistent with mobilization of Mesoproterozoic crust of passive margin if the Lu/Hf = 0.015 (Fig. 12a). According to our present understanding, the zircon populations of 950–850 Ma and

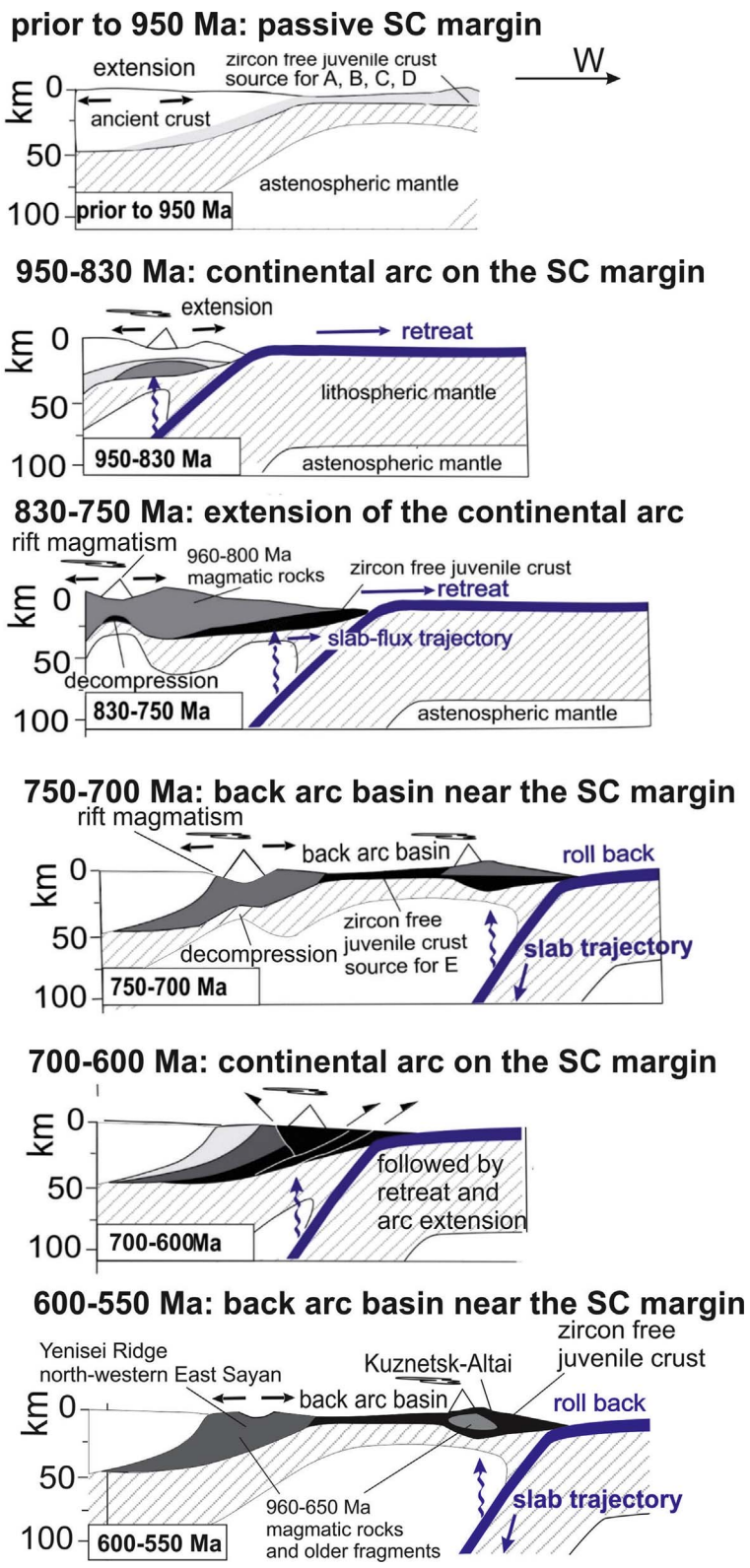

Fig. 14. A tectonic model drawn using Collins (2002) and Priyatkina et al. (2017) shows the development of the Neoproterozoic accretionary orogen along the western margin of the Siberian Craton through five main phases: establishing mafic underplated crust of a passive margin (late Mesoproterozoic); establishing continental arc allowing for generation of zircon-bearing magmas at the expense of juvenile and evolved material (950–850 Ma); progressive arc extension during (800–750 Ma), followed by trench retreat, ribbon rift-off and back-arc basin opening (750–700 Ma); arc accretion and back arc closure results in generation of juvenile zircon bearing magmas (700–600 Ma); a new phase of roll-back and arc accretion followed (600–500 Ma).

900–850 Ma (Fig. 12b) can be related to extended fractionation of two magmatic systems, represented by the S-I type Teya-Yeruda granite gneiss domes and granitoids of the Garevka Massif that have features transitional between the S- and A-type granites. In the north-western East Sayan the analogue of the Central Angara magmatic arc is possibly represented by the Arzibei (Turkina et al., 2004) and the Kuvai (Bezzubtsev et al., 2008b) terranes. Simultaneously, the older sedimentary basement of the CAT undergoes andalusite-sillimanite, kyanite-sillimanite metamorphism, high-P amphibolite metamorphism and migmatization associated with growth of zircon, monazite, xenotime (Likhanov and Reverdatto, 2014a,b; Kuzmichev and Sklyarov, 2016). Moreover, in the EAT, the deposition of the ca. 900–850 Ma siliciclastic Krasnogor Formation may have been associated with erosion of this arc. Subsequent uplift and unroofing of the Siberian margin

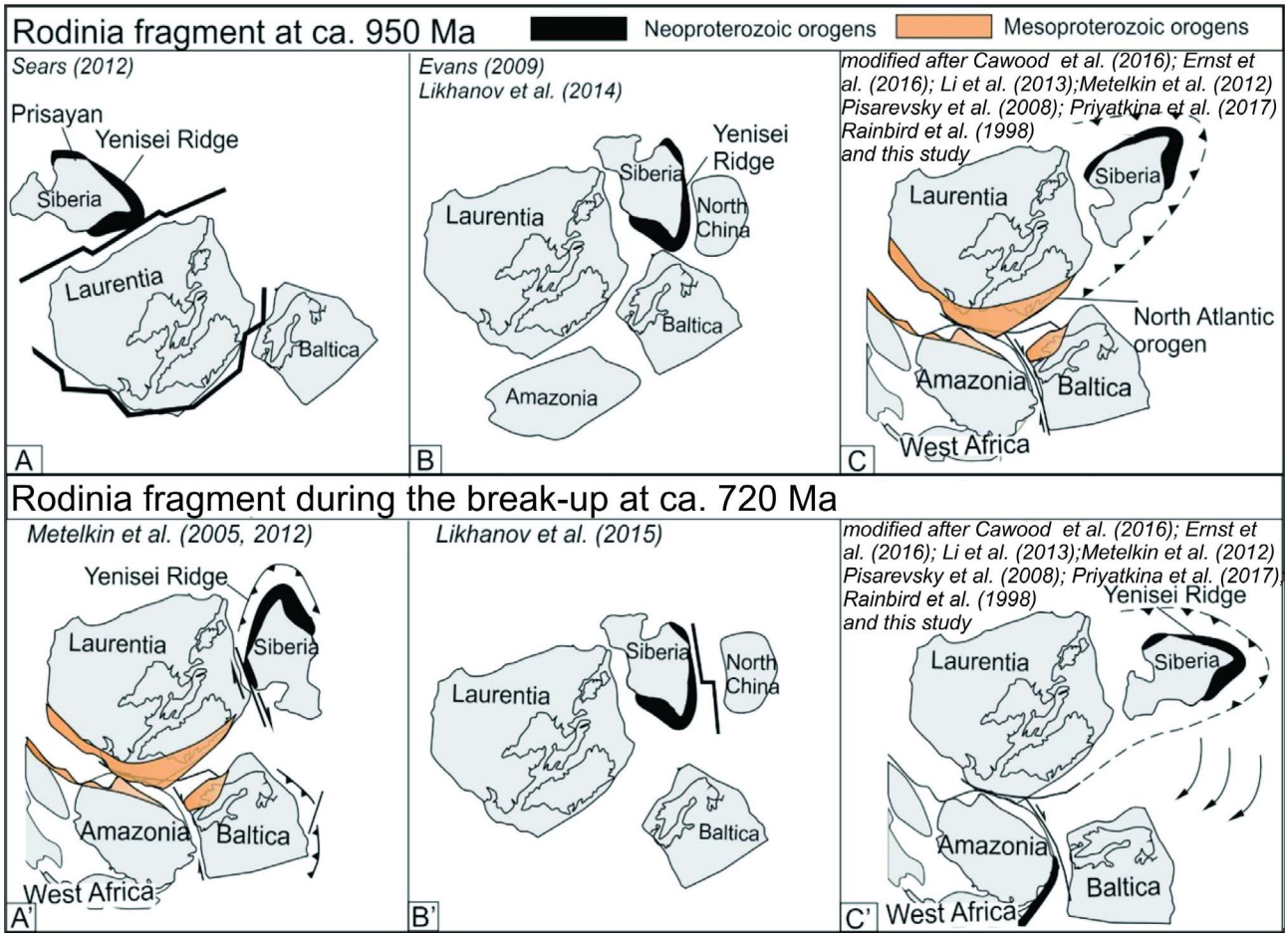

Fig. 15. Various models showing possible Laurentia-Siberia-Baltica connections within the Rodinia supercontinent and during Rodinia break-up (see also supplementary file in Ernst et al. (2016), Khudoley et al. (2015) or Priyatkina et al. (2017) for a more detailed review): a after Sears (2012); B after Evans (2009) followed by Likhanov et al. (2014); C after Cawood et al. (2016), Ernst et al. (2016), Li et al. (2013), Metelkin et al. (2012), Pisarevsky et al. (2008), Priyatkina et al. (2017), Rainbird et al. (1998); and this study; A′ after Metelkin et al. (2012), B′ after Likhanov and Reverdatto (2015), C′ after Cawood et al. (2016), Ernst et al. (2016), Li et al. (2013), Metelkin et al. (2012), Pisarevsky et al. (2008), Priyatkina et al. (2017), Rainbird et al. (1998) and this study.

at ca. 850–800 Ma is reflected by closure of K-Ar isotopic systems within the EAT, CAT and the Turukhansk Uplift and the extensive depositional hiatus (Fig. 12). Active continental margin setting of the CAT is consistent with geodynamic models of Vernikovsky et al. (2009) and Kuzmichev and Sklyarov (2016).

7.3. Phase 2 (840–750 Ma)

Progressive extension of the continental arc produces a shift towards more positive εHf (T) values, consistent with emplacement of relatively juvenile A-type magmas and bimodal volcanic suites of Garevka, Glushikha, Vorogovka, Khareuzhikha, Chirimba, Ayakhta and Lendakha (Vernikovskaya et al., 2003, 2006; Vernikovskaya et al., 2007).

7.4. Phase 3 (750–700 Ma)

Progressive trench retreat results in opening of a back-arc basin along the western SC margin, broadly reflected in development of rift basins within the EAT, CAT and the Prisayan Uplift, accompanied by emplacement of mafic dike swarms, bimodal volcanism (e.g., Gladkochub et al., 2010b; Nozhkin et al., 2013; Sklyarov et al., 2002) and medium-T medium-P metamorphism in the Angara-Kan terrane (Nozhkin et al., 2016b). An ongoing zircon production during this period suggests a setting similar to modern Japan or New Zealand outboard the margin. Its fragments maybe represented by the calc-alkaline rock association of the Kuvai terrane which Rb-Ar and Sm-Nd age estimates vary between 770 and 720 Ma (Bezzubtsev et al., 2008a) and the Sarkhoi volcanics (Kuzmichev and Larionov, 2011).

Previously, this evolutionary interval has been considered as rifting stage associated with a break-up of Siberia from Rodinia (Likhanov et al., 2014; Vernikovsky et al., 2009; Nozhkin et al., 2008).

7.5. Phase 5 (700–630 Ma)

Further growth of the continental arc near the western margin of the SC is reflected by the juvenile 700–630 Ma zircon population, with slope of ~Lu/Hf = 0.22 suggests its 800–700 Ma ensimatic basement (Fig. 12b). Fragments of this age are commonly referred to as the Isakovka-Predivinsk (IPT) terrane (Kuzmichev et al., 2008; Vernikovsky et al., 1999, 2001, 2003). Arc accretion occurred at ~630 Ma as evidenced by widespread metamorphism in the Angara belt (Nozhkin et al., 2007). Following arc extension was associated with subalkaline and alkaline magmatism (Nozhkin et al., 2001, 2003; Romanova et al., 2012; Vernikovskaya et al., 2013; Vernikovsky et al., 2008), formation of the major unconformity and post-accretionary sedimentary successions (Section 5.2).

7.6. Phase 6 (post-600 Ma)

The majority of researchers (Buslov et al., 2002; Glorie et al., 2011; Safonova, 2014; Ota et al., 2007; Chen et al., 2015) consider that a later

560–515 Ma magmatic arc of Kuznetsk and Gorny Altai formed on the margin of the SC and was accreted by 500 Ma. The zircon population recovered from the arc's erosional products are characterised by εHf (T) of 0 to +15 (Fig. 13a). Two main evidences favour formation of this arc near the SC: (1) Cambrian and Ordovician arc-related rocks have Neoproterozoic basement (Rudnev et al., 2006, 2013), and cut across the Neoproterozoic basement of the north-western East Sayan (Turkina et al., 2007). This basement was a part of the western SC margin at least since the end of the Neoproterozoic (Section 6.3 and references therein), (2) Formation of the early Paleozoic subduction-accretion complex on the western SC margin is evidenced from similarities of detrital zircon populations from synorogenic sedimentary deposits of Gorny Altai (Glorie et al., 2011; Chen et al., 2015) and the Siberian platform (Glorie et al., 2014). Broadly, in the Neoproterozoic to Early Paleozoic, Hf in zircon arrays of the western SC margin show evolutionary trends towards more positive epsilon Hf values (Fig. 13a), similar to the trends shown for typical accretionary orogens by Collins et al. (2011).

8. Implications for the Neoproterozoic supercontinental reconstructions

8.1. Implications for Rodinia reconstructions

In respect to position of the western SC margin, Rodinia models can be broadly subdivided into three main groups (Fig. 15), including (A) the models that consider juxtaposition between the northern SC and western Laurentia along a transform fault (Sears, 2012), (B) the models that consider an internal to Rodinia position of northern and western SC margins (Evans, 2009; Likhanov et al., 2014), (C) the models that consider external to Rodinia position of northern and western SC margins (Cawood et al., 2016; Ernst et al., 2016; Li et al., 2013; Metelkin et al., 2012; Pisarevsky et al., 2008; Rainbird et al., 1998). Group A models are not supported by geological evidence (Priyatkina et al., 2017 and ref. therein) because they do not allow for the inferred subduction zone near the northern margin of the SC at ~950 Ma. For similar reason, Group B models requiring an intracratonic position for the western SC margin in the early Neoproterozoic are not supported by this study. Also, there is no reliable geological or geochronological evidence to support the existence of a *sensu stricto* Mesoproterozoic or Grenville orogen (Likhanov et al., 2014, 2012) which could potentially suture western Siberia and North China (Group B models): the only known Mesoproterozoic granitoids in the area are the Nemtikha and Cherniya Zima felsic components of bimodal suites dated at ~1380 Ma and ~1530 Ma, respectively (Gladkochub et al., 2002; Popov et al., 2010). Similarly, the existence of a Mesoproterozoic orogenic belt along the western SC cannot be postulated simply based on ID TIMS zircon ages of ca. 1100–1000 Ma derived from the Teya granite-gneiss domes, because these domes bear several zircon populations that range between 1100 Ma and 850 Ma, and the origin of the older grains is uncertain (Nozhkin et al., 1999). Nonetheless, Mesoproterozoic pre-unconformity succession was subjected to medium-T low-P metamorphism, which geodynamic nature requires further investigation (see Section 7).

Consistent with configurations suggested in the Group C models (Fig. 15), the margins of western Siberia, northern Siberia and north-eastern Laurentia share many similarities in their geological evolution at ca. 1000–750 Ma. In the northern and western SC, the fragments of Siberian Mesoproterozoic passive margin or a rift basin are represented by the ca. 1650–1380 Ma Oktyabr'–Zhdanov Group and the ca. 1650–1000 Ma Sukhopit Group, which comprises up to 5 km thick succession of carbonate and mature siliciclastic rock units, supplied from the northern SC and western SC, respectively (e.g., Priyatkina et al., 2016, 2017). In the north-eastern part of Laurentia their correlatives are best exemplified by the Krummedal succession of East Greenland (Cawood et al., 2010, and ref. therein). The 1700–970 Ma magmatic gap, characteristic of the overall Proterozoic detrital zircon signatures of the northern and western SC margins (Fig. 12, see also Fig. 11 in Priyatkina et al., 2017), indicates that these margins were a divergent plate boundary throughout the Mesoproterozoic, until their transformation from passive into active occurred at 980–970 Ma, coeval with initiation of Valhalla orogen.

8.2. Implications for Rodinia break-up

Several models (Fig. 15) consider the late Neoproterozoic relationship between Laurentia, Siberia and Baltica, or its absence. Group A′ models (e.g., Ernst et al., 2016; Metelkin et al., 2010, 2012) imply that Siberia was connected to northern Laurentia via a rift basin, which fragments are currently represented by the Karagas Group. Despite being consistent with the developing accretionary orogen of the Yenisey Ridge, this model does not allow for developing the oceanic and continental arcs in the north-western East Sayan, which are likely to have the peri-Siberian origin (Section 6.3). Group B′ models consider the opening of an Atlantic-style rift basin near the western margin of Siberia at ca. ~720 Ma, based on the emplacement of rift-related volcanic rocks and dike swarms (e.g., Likhanov and Reverdatto, 2015). However, this scenario does not allow for continuous zircon production during 950–600 Ma (Section 7). Finally, in our preferred interpretation (Group C′ model), it is followed that by ca. 720 Ma SC evolved as an independent landmass (e.g., Pavlov et al., 2015; Pisarevsky et al., 2013) and was surrounded by subduction zones at least from the present western and northern sides (Priyatkina et al., 2017, and this study). In this interpretation, extensional environments responsible for rift-related magmatism along the south-western SC margin at ~800–700 Ma are seen as the result of coexisting rifting (between southern Siberia and northern Laurentia), and extension caused by the retreat of a continental ribbon and formation of back arc basins near the south-western SC.

9. Conclusions

(1) The Neoproterozoic to Lower Cambrian sandstones in the Yenisey Ridge (the Taseeva basin) contain abundant 2.7–2.5 Ga, 2.0–1.75 Ga and 0.95–0.57 Ga erosional products, and in the sandstones of the Prisayan Uplift slightly different detrital zircon ages of 3.0–2.5 Ga, 2.2–1.8 Ga and 0.95–0.65 Ma are common.
(2) The sandstones collected below the major Ediacaran unconformity surface received detritus from proximal Archean and Paleoproterozoic crustal units of the western SC margin, whereas the post-unconformity upper Ediacaran to Lower Cambrian sandstones formed by cannibalization of the underlying sedimentary rocks and at the expense of proximal Neoproterozoic arc-related igneous suites, located in the western fringe of the SC.
(3) Hf isotopic and geological evidence favours the existence of a long-term Neoproterozoic subduction zone near the western SC margin, a part of a larger peri-Rodinian subduction system.

Acknowledgements

Financial support was provided by the University of Newcastle PhD scholarship, Australian Research Council Discovery Project 120104004, Grant of the Ministry of Science and Education of the Russian Federation # 14.Z50.31.0017, St. Petersburg State University research grant# 3.38.137.2014 and by state assignment project № 03300-2016-0015. This article is a contribution to IGCP648. N. Priyatkina thanks A. D. Nozhkin for his personal communication and V.B. Ershova for providing samples 1-EB-1, 3-EB-1 and 8-EB-1. Comments made by Dr. Richard Ernst, Dr Sergei Pisarevsky and Dr Randall Parrish (the Editor) greatly improved this manuscript.

Appendix A. Supplementary data

Supplementary data associated with this article can be found, in the online version, at http://dx.doi.org/10.1016/j.precamres.2017.12.014.

References

Abrajevitch, A., Van der Voo, R., Bazhenov, M.L., Levashova, N.M., McCausland, P.J.A., 2008. The role of the Kazakhstan orocline in the late Paleozoic amalgamation of Eurasia. Tectonophysics 455, 61–76.

Bennett, V.C., Brandon, A.D., Nutman, A.P., 2007. Coupled ^{142}Nd-^{143}Nd isotopic evidence for Hadean mantle dynamics. Science 318, 1907–1910.

Berezii, A.E., Krus', Z.I., Shevchenko, V.V., 1973. Geological map of the USSR. Scale 1:200,000. Sheet O-47-XIII. Aerogeologiya, Moscow [In Russia].

Bethune, K.M., 2015. The Rae craton of Laurentia/Nuna: a tectonically unique entity providing critical insights into the concept of Precambrian supercontinental cyclicity, American Geophysical Union, Fall Meeting 2015, abstract #T13A-2980.

Bezzubtsev, V.V., Perfilova, O.Yu., 2008. Geological Map of Russian Federation. Scale 1: 1 000 000. Sheet N-46 (Abakan). VSEGEI, St.-Petersburg [In Russian].

Bezzubtsev, V.V., Makhlaev, M.L., Kirichenko, V.T., 2008a. Explanatary Note to Geological Map of Russian Federation (sheet N-46 1:1,000,000, Abakan). VSEGEI, St.-Petersburg, pp. 390 [In Russian].

Bezzubtsev, V.V., Makhlaev, M.L., Kirichenko, V.T., Perfilova, O.Yu., Yurkevich, L.G., Markovich, L.A., Zuev, V.K., Rumyantsev, N.N., Datsenko, V.M., Dyatlova, I.N., 2008b. Explanatory Note to the Geological Map of Russian Federation (sheet M-46 1:1,000,000, Kyzyl). VSEGEI, St.-Petersburg, pp. 316 [In Russian].

Blichert-Toft, J., Albarède, F., 2008. Hafnium isotopes in Jack Hills zircons and the formation of the Hadean crust. Earth Planet. Sci. Lett. 265, 686–702.

Buslov, M.M., Saphonova, I.Y., Watanabe, T., Obut, O.T., Fujiwara, Y., Iwata, K., Semakov, N.N., Sugai, Y., Smirnova, L.V., Kazansky, A.Y., 2001. Evolution of the Paleo-Asian Ocean (Altai-Sayan Region, Central Asia) and collision of possible Gondwana-derived terranes with the southern marginal part of the Siberian continent. Geosci. J. 5, 203–224.

Buslov, M.M., Watanabe, T., Saphonova, I.Y., Iwata, K., Travin, A., Akiyama, M., 2002. A Vendian-Cambrian arc system of the Siberian continent in Gorny Altai (Russia, Central Asia). Gondwana Res. 5, 781–800.

Buslov, M.M., Geng, H., Travin, A.V., Otgonbaatar, D., Kulikova, A.V., Ming, C., Stijn, G., Semakov, N.N., Rubanova, E.S., Abildaeva, M.A., Voitishek, E.E., Trofimova, D.A., 2013. Tectonics and geodynamics of Gorny Altai and adjacent structures of the Altai-Sayan folded area. Russ. Geol. Geophys. 54, 1250–1271.

Cawood, P.A., Strachan, R., Cutts, K., Kinny, P.D., Hand, M., Pisarevsky, S., 2010. Neoproterozoic orogeny along the margin of Rodinia: Valhalla orogen, North Atlantic. Geology 38, 99–102.

Cawood, P.A., Strachan, R.A., Pisarevsky, S.A., Gladkochub, D.P., Murphy, J.B., 2016. Linking collisional and accretionary orogens during Rodinia assembly and breAKTp: implications for models of supercontinent cycles. Earth Planet. Sci. Lett. 449, 118–126.

Chen, M., Sun, M., Buslov, M.M., Cai, K., Zhao, G., Zheng, J., Rubanova, E.S., Voytishek, E.E., 2015. Neoproterozoic–middle Paleozoic tectono-magmatic evolution of the Gorny Altai terrane, northwest of the Central Asian Orogenic Belt: constraints from detrital zircon U-Pb and Hf-isotope studies. Lithos 233, 223–236.

Collins, W.J., Belousova, E.A., Kemp, A.I.S., Murphy, J.B., 2011. Two contrasting Phanerozoic orogenic systems revealed by hafnium isotope data. Nat. Geosci. 4, 333–337.

Collins, W.J., 2002. Hot orogens, tectonic switching, and creation of continental crust. Geology 30, 535–538.

Dhuime, B., Hawkesworth, C., Cawood, P., 2011. When Continents formed. Science 331, 154–155.

Dickinson, W.R., Gehrels, G.E., 2009. Use of U-Pb ages of detrital zircons to infer maximum depositional ages of strata: a test against a Colorado plateau mesozoic database. Earth Planet. Sci. Lett. 288, 115–125.

Dobretsov, N.L., Buslov, M.M., 2007. Late Cambrian-Ordovician tectonics and geodynamics of Central Asia. Russ. Geol. Geophys. 48, 71–82.

Donskaya, T.V., Gladkochub, D.P., Mazukabzov, A.M., Wingate, M.T.D., 2014. Early Proterozoic postcollisional granitoids of the Biryusa block of the Siberian craton. Russ. Geol. Geophys. 55, 812–823.

Ernst, R.E., Hamilton, M.A., Soderlund, U., Hanes, J.A., Gladkochub, D.P., Okrugin, A.V., Kolotilina, T., Mekhonoshin, A.S., Bleeker, W., LeCheminant, A.N., Buchan, K.L., Chamberlain, K.R., Didenko, A.N., 2016. Long-lived connection between southern Siberia and northern Laurentia in the Proterozoic. Nat. Geosci. 9, 464–469.

Evans, D.A.D., 2009. The palaeomagnetically viable, long-lived and all-inclusive Rodinia supercontinent reconstruction. Geological Society, London, Special Publications 327, pp. 371–404.

Filippov, Y.F., 2017. The Fore-Yenisey sedimentary basin: seismic-geological model and geodynamic history. Russ. Geol. Geophys. 58, 371–383.

Galimova, T.F., Pashkova, A.G., 2012. Geological Map of Russian Federation. Scale 1:1,000,000. Sheet N-47 (Nizhneudinsk). VSEGEI, St. Petersburg.

Galimova, T.F., Pashkova, A.G., Povarintseva, S.A., Perfiliev, V.V., 2012. Explanatory Note to the State Geological Map of Russian Federation (Sheet N-47, Nizhneudinsk). VSEGEI, St. Petersburg, pp. 653.

Geng, Y., Du, L., Ren, L., 2012. Growth and reworking of the early Precambrian continental crust in the North China Craton: constraints from zircon Hf isotopes. Gondwana Res. 21, 517–529.

Gladkochub, D., Donskaya, T., Mazukabzov, A., Sklyarov, E., Ponomarchuk, V., Stanevich, A., 2002. The Urik-Iya graben of the Sayan ledge of the Siberian craton: new geochronological data and geodynamic implications. Doklady Rossijskaya Akademiya Nauk 386, 72–77.

Gladkochub, D., Donskaya, T., Mazukabzov, A., Sal'nikova, E., Sklyarov, E., Yakovleva, S., 2005. The age and geodynamic interpretation of the Kitoi granitoid complex (southern Siberian craton). Russ. Geol. Geophys. 46, 1121–1133.

Gladkochub, D.P., Wingate, M.T.D., Pisarevsky, S.A., Donskaya, T.V., Mazukabzov, A.M., Ponomarchuk, V.A., Stanevich, A.M., 2006. Mafic intrusions in southwestern Siberia and implications for a Neoproterozoic connection with Laurentia. Precambr. Res. 147, 260–278.

Gladkochub, D.P., Donskaya, T.V., Wingate, M.T.D., Mazukabzov, A.M., Pisarevsky, S.A., Sklyarov, E.V., Stanevich, A.M., 2010a. A one-billion-year gap in the Precambrian history of the southern Siberian Craton and the problem of the Transproterozoic supercontinent. Am. J. Sci. 310, 812–825.

Gladkochub, D.P., Pisarevsky, S.A., Donskaya, T.V., Ernst, R.E., Wingate, M.T.D., Söderlund, U., Mazukabzov, A.M., Sklyarov, E.V., Hamilton, M.A., Hanes, J.A., 2010b. Proterozoic mafic magmatism in Siberian craton: an overview and implications for paleocontinental reconstruction. Precambr. Res. 183, 660–668.

Glebovitsky, V.A., Khil'tova, V.Y., Kozakov, I.K., 2008. Tectonics of the Siberian Craton: interpretation of geological, geophysical, geochronological, and isotopic geochemical data. Geotectonics 42, 8–20.

Glorie, S., De Grave, J., Buslov, M.M., Zhimulev, F.I., Izmer, A., Vandoorne, W., Ryabinin, A., Van den haute, P., Vanhaecke, F., Elburg, M.A., 2011. Formation and Palaeozoic evolution of the Gorny-Altai–Altai-Mongolia suture zone (South Siberia): Zircon U/Pb constraints on the igneous record. Gondwana Res. 20, 465–484.

Glorie, S., De Grave, J., Buslov, M.M., Zhimulev, F.I., Safonova, I.Y., 2014. Detrital zircon provenance of early Palaeozoic sediments at the southwestern margin of the Siberian Craton: insights from U-Pb geochronology. J. Asian Earth Sci. 82, 115–123.

Goldstein, A., 1987. Use and abuse of crust-formation ages. Geology 15, 893–895.

Gorokhov, I.M., Semikhatov, M.A., Baskakov, A.V., Kutyavin, E.P., Mel'nikov, N.N., Sochava, A.V., Turchenko, T.L., 1995. Sr isotopic composition of Vendian and Lower Cambrian carbonate rocks in Siberia. Stratigr. Geol. Correl. 3, 3–33 [In Russian].

Grazhdankin, D.V., Kontorovich, A.E., Kontorovich, V.A., Saraev, S.V., Filippov, Y.F., Efimov, A.S., Karlova, G.A., Kochnev, B.B., Nagovitsin, K.E., Terleev, A.A., Fedyanin, G.O., 2015. Vendian of the Fore-Yenisey sedimentary basin (southeastern West Siberia). Russ. Geol. Geophys. 56, 560–572.

Griffin, W.L., Wang, X., Jackson, S.E., Pearson, N.J., O'Reilly, S.Y., Xu, X., Zhou, X., 2002. Zircon chemistry and magma mixing, SE China: in-situ analysis of Hf isotopes, Tonglu and Pingtan igneous complexes. Lithos 61, 237–269.

Hoskin, P.W.O., Schaltegger, U., 2003. The composition of zircon and igneous and metamorphic petrogenesis. In: Hanchar, J.M., Hoskin P.W.O., (Eds.), Zircon, pp. 27–62. (Reviews in Mineralogy and Geochemistry, vol. 53).

Johansson, Å., 2014. From Rodinia to Gondwana with the 'SAMBA' model—A distant view from Baltica towards Amazonia and beyond. Precambr. Res. 244, 226–235.

Kachevsky, L.K., Zuev, V.K., 2009. Geological Map of Russian Federation. Scale 1:1,000,000. Sheet 0-46. VSEGEI, St. Petersburg.

Kalinovsky, A.L., Smolyanets, B.G., 1965. Geological Map of the USSR. Scale 1: 200,000. Sheet N-47-III. VSEGEI, St. Petersburg.

Khabarov, E.M., Varaksina, I.V., 2011. The structure and depositional environments of Mesoproterozoic petroliferous carbonate complexes in the western Siberian craton. Russ. Geol. Geophys. 52, 923–944.

Kheraskova, T.N., Kaplan, S.A., Galuev, V.I., 2009. Structure of the Siberian platform and its western margin in the Riphean-Early Paleozoic. Geotectonics 43, 115–132.

Khudoley, A., Chamberlain, K., Ershova, V., Sears, J., Prokopiev, A., MacLean, J., Kazakova, G., Malyshev, S., Molchanov, A., Kullerud, K., Toro, J., Miller, E., Veselovskiy, R., Li, A., Chipley, D., 2015. Proterozoic supercontinental restorations: constraints from provenance studies of Mesoproterozoic to Cambrian clastic rocks, eastern Siberian Craton. Precambr. Res. 259, 78–94.

Kirichenko, V.T., Zuev, V.K., Perfilova, O.Yu., Senovskaya, O.V., Smokitina, I.V., Markovich, L.A., Borodin, V.P., Mironyuk, E.P., 2012. Explanatory Note to Geological Map of Russian Federation (Sheet O-47 in Scale 1: 1 000,000). VSEGEI, St. Petersburg, pp. 470 [In Russian].

Kochnev, B.B., Karlova, G.A., 2010. New data on biostratigraphy of the Vendian Nemakit-Daldynian stage in the southern Siberian platform. Stratigr. Geol. Correl. 18, 492–504.

Komarevsky, V.T., Zhukov, N.V., 1964. Geological Map of the USSR. Scale 1: 200 000. Sheet N-47-II. VSEGEI, St. Petersburg [In Russian].

Kovrigina, E.K., Podgornaya, N.S., Guriev, A.G., Semenov, Yu.G., Semerikov, A.A., 1974. Geological Map of the USSR. Scale 1: 1,000,000. Sheet O-46 (47). VSEGEI, St. Petersburg [In Russian].

Kozlov, P.S., Likhanov, I.I., Reverdatto, V.V., Zinoviev, S.V., 2012. Tectonometamorphic evolution of the Garevka polymetamorphic complex (Yenisey Ridge). Russ. Geol. Geophys. 53, 1133–1149.

Kröner, A., Kovach, V., Belousova, E., Hegner, E., Armstrong, R., Dolgopolova, A., Seltmann, R., Alexeiev, D.V., Hoffmann, J.E., Wong, J., Sun, M., Cai, K., Wang, T., Tong, Y., Wilde, S.A., Degtyarev, K.E., Rytsk, E., 2014. Reassessment of continental growth during the accretionary history of the Central Asian Orogenic Belt. Gondwana Res. 25, 103–125.

Kuzmichev, A.B., Larionov, A.N., 2011. The Sarkhoi Group in East Sayan: Neoproterozoic (~770–800 Ma) volcanic belt of the Andean type. Russ. Geol. Geophys. 52, 685–700.

Kuzmichev, A.B., Sklyarov, E.V., 2016. The Precambrian of Transangaria, Yenisey Ridge (Siberia): Neoproterozoic microcontinent, Grenville-age orogen, or reworked margin of the Siberian craton? J. Asian Earth Sci. 115, 419–441.

Kuzmichev, A.B., Paderin, I.P., Antonov, A.V., 2008. Late Riphean Borisikha ophiolite (Yenisey Ridge): U-Pb zircon age and tectonic setting. Russ. Geol. Geophys. 49, 883–893.

Letnikova, E.F., Kuznetsov, A.B., Vishnevskaya, I.A., Veshcheva, S.V., Proshenkin, A.I., Geng, H., 2013. The Vendian passive continental margin in the southern Siberian Craton: geochemical and isotopic (Sr, Sm–Nd) evidence and U-Pb dating of detrital zircons by the LA-ICP-MS method. Russ. Geol. Geophys. 54, 1177–1194.
Levashova, N.M., Gibsher, A.S., Meert, J.G., 2011. Precambrian microcontinents of the Ural-Mongolian Belt: new paleomagnetic and geochronological data. Geotectonics 45, 51–70.
Li, Z.-X., Evans, D.A.D., Halverson, G.P., 2013. Neoproterozoic glaciations in a revised global palaeogeography from the breakup of Rodinia to the assembly of Gondwanaland. Sed. Geol. 294, 219–232.
Likhanov, I.I., Reverdatto, V.V., 2014a. Geochemistry, age, and petrogenesis of rocks from the Garevka metamorphic complex, Yenisey Ridge. Geochem. Int. 52, 1–21.
Likhanov, I.I., Reverdatto, V.V., 2014b. P-T-t constraints on the metamorphic evolution of the Transangarian Yenisei Ridge: geodynamic and petrological implications. Russ. Geol. Geophys. 55, 299–322.
Likhanov, I.I., Reverdatto, V.V., 2015. Evidence of Middle Neoproterozoic extensional tectonic settings along the western margin of the Siberian craton: implications for the breakup of Rodinia. Geochem. Int. 53, 671–689.
Likhanov, I.I., Reverdatto, V.V., Kozlov, P.S., Vershinin, A.E., 2011. The Teya polymetamorphic complex in the Transangarian Yenisei Ridge: an example of metamorphic superimposed zoning of low- and medium-pressure facies series. Dokl. Earth Sci. 436, 213–218.
Likhanov, I.I., Reverdatto, V.V., Kozlov, P.S., 2012. U-Pb and $^{40}Ar/^{39}Ar$ evidence for Grenvillian activity in the Yenisey Ridge during formation of the Teya metamorphic complex. Geochem. Int. 50, 551–557.
Likhanov, I.I., Reverdatto, V.V., Zinov'ev, S.V., Nozhkin, A.D., 2013. Age of blastomilonites of the Yenisei regional shear zone as evidence of the Vendian accretionary-collision events at the western margin of the Siberian Craton. Doklady Earth Sci. 450, 489–493.
Likhanov, I.I., Nozhkin, A.D., Reverdatto, V.V., Kozlov, P.S., 2014. Grenville tectonic events and evolution of the Yenisei Ridge at the western margin of the Siberian Craton. Geotectonics 48, 371–389.
Linnemann, U., Gerdes, A., Hofmann, M., Marko, L., 2014. The Cadomian Orogen: Neoproterozoic to Early Cambrian crustal growth and orogenic zoning along the periphery of the West African Craton-Constraints from U-Pb zircon ages and Hf isotopes (Schwarzburg Antiform, Germany). Precambr. Res. 244, 236–278.
Liu, A.G., Brasier, M.D., Bogolepova, O.K., Raevskaya, E.G., Gubanov, A.P., 2013. First report of a newly discovered Ediacaran biota from the Irkineeva Uplift, East Siberia. Newsl. Stratigr. 46, 95–110.
Melnikov, N.V., Yakshin, M.S., Shishkin, B.B., Efimov, A.O., Karlova, G.A., Kilkina, L.I., Konstantinova, L.N., Kochnev, B.B., Kraevskiy, B.G., Melnikov, P.N., Nagovitsin, K.E., Postnikov, A.A., Ryabkova, L.V., Terleev, A.A., Khabarov, E.M., 2005. Stratigraphy of Oil and Gas Basins of SIBERIA. Riphean and Vendian of Siberian Platform and its Plaited Border. Novosibirsk, Geo, pp. 428 [In Russian].
Merdith, A.S., Collins, A.S., Williams, S.E., Pisarevsky, S., Foden, J.F., Archibald, D., Blades, M.L., Alessio, B.L., Armistead, S., Plavsa, D., 2017. A full-plate global reconstruction of the Neoproterozoic. Gondwana Res. 50, 84–134.
Metelkin, D.V., Blagovidov, V.V., Kazansky, A.Y., 2010. The history of the Karagas Supergroup evolution in the Biryusa region: synthesis of paleomagnetic and sedimentological data. Russ. Geol. Geophys. 51, 868–884.
Metelkin, D., Ernst, R.E., Hamilton, M., 2011. A ca. 1640 Ma mafic magmatic event in southern Siberia, and links with northern Laurentia, Geological Society of America Annual Meeting (9–12 October 2011), abstract no. 101-1, Minneapolis, USA.
Metelkin, D.V., Vernikovsky, V.A., Kazansky, A.Y., 2012. Tectonic evolution of the Siberian paleocontinent from the Neoproterozoic to the Late Mesozoic: paleomagnetic record and reconstructions. Russ. Geol. Geophys. 53, 675–688.
Motova, Z.L., Gladkochub, D.P., Donskaya, T.V., Stanevich, A.M., Mazukabzov, A.M., 2013. Age of detrital zircons and lithochemistry of siliciclastic Shangulezh Formation of the Karagas Group, In: Sklyarov, E.V. (Ed.), Proceedings of Meeting «Geodynamic evolution of the Central Asian Orogenic Belt lithosphere (from ocean to continent)». V. 11. Irkutsk, IZK SO RAN, pp. 171–172. [In Russian].
Motova, Z.L., Donskaya, T.V., Gladkochub, D.P., 2016. The composition and reconstruction of the source area for the late Precambrian terrigenous rocks of the Oselkovaya series (Biryusa Prisayanie). Geodyn. Tectonophys. (Inst. Earth's Crust RAS) 7 (4), 625–649 [In Russian].
Nozhkin, A., Turkina, O., Bibikova, E., Terleev, A., Khomentovsky, V., 1999. Riphean granite-gneiss domes of the Yenisey Range: geological structure and U-Pb isotopic age. Geol. Geofiz. 40, 1305–1313 [In Russian].
Nozhkin, A., Turkina, O., Bibikova, E., Ponomarchuk, V., 2001. Structure, composition, and formation conditions of metasedimentary-volcanogenic complexes of the Kan greenstone belt: (Northwestern Sayan region). Geologiya i Geofizika 42, 1058–1078 [In Russian].
Nozhkin, A., Bibikova, E., Turkina, O., Ponomarchuk, V., 2003. U-Pb, Ar-Ar, and Sm-Nd isotope-geochronological study of porphyritic subalkalic granites of the Taraka pluton (Yenisey Range). Geologiya i Geofizika 44, 879–889 [In Russian].
Nozhkin, A.D., Turkina, O.M., Sovetov, Y.K., Travin, A.V., 2007. The Vendian accretionary event in the southwestern margin of the Siberian Craton. Dokl. Earth Sci. 415, 869–873.
Nozhkin, A.D., Turkina, O.M., Bayanova, T.B., Berezhnaya, N.G., Larionov, A.N., Postnikov, A.A., Travin, A.V., Ernst, R.E., 2008. Neoproterozoic rift and within-plate magmatism in the Yenisey Ridge: implications for the breakup of Rodinia. Russ. Geol. Geophys. 49, 503–519.
Nozhkin, A.D., Borisenko, A.S., Nevol'ko, P.A., 2011. Stages of Late Proterozoic magmatism and periods of Au mineralization in the Yenisei Ridge. Russ. Geol. Geophys. 52, 124–143.
Nozhkin, A.D., Kachevskii, L.K., Dmitrieva, N.V., 2013. The Late Neoproterozoic rift-related metarhyolite–basalt association of the Glushikha trough (Yenisey Ridge): petrogeochemical composition, age, and formation conditions. Russ. Geol. Geophys. 54, 44–54.
Nozhkin, A.D., Popov, N.V., Dmitrieva, N.V., Storozhenko, A.A., Vasil'ev, N.F., 2015a. Neoproterozoic collisional S-type granitoids of the Yenisey Ridge: petrogeochemical composition and U-Pb, Ar-Ar, and Sm-Nd isotope data. Russ. Geol. Geophys. 56, 689–695.
Nozhkin, A.D., Turkina, O.M., Dmitrieva, N.V., Likhanov, I.I., 2015b. Age and P-T parameters of metamorphism of metaterrigenous-carbonate deposits of the Derba block (East Sayan). Dokl. Earth Sci. 461, 390–393.
Nozhkin, A.D., Turkina, O.M., Likhanov, I.I., Dmitrieva, N.V., 2016. Late Paleoproterozoic volcanic associations in the southwestern Siberian craton (Angara-Kan block). Russ. Geol. Geophys. 57, 247–264.
Nozhkin, A.D., 2009. Precambrian of the southwestern Siberian cratonic margin. Izvestiya Tomsk Polytechnic University 314, 5–16 [In Russian].
Ota, T., Utsunomiya, A., Uchio, Y., Isozaki, Y., Buslov, M.M., Ishikawa, A., Maruyama, S., Kitajima, K., Kaneko, Y., Yamamoto, H., Katayama, I., 2007. Geology of the Gorny Altai subduction–accretion complex, southern Siberia: tectonic evolution of an Ediacaran-Cambrian intra-oceanic arc-trench system. J. Asian Earth Sci. 30, 666–695.
Pavlov, V.E., Shatsillo, A.V., Petrov, P.Y., 2015. Paleomagnetism of the upper Riphean deposits in the Turukhansk and Olenek uplifts and Uda Pre-Sayan region and the Neoproterozoic drift of the Siberian Platform: Izvestiya. Phys. Solid Earth 51, 716–747.
Payne, J.L., McInerney, D.J., Barovich, K.M., Kirkland, C.L., Pearson, N.J., Hand, M., 2016. Strengths and limitations of zircon Lu-Hf and O isotopes in modelling crustal growth. Lithos 248–251, 175–192.
Petrov, P.Yu., 2006. Riphean basins of the Turukhansk Uplift of Siberia: origin, geological history and importance of biological component in sedimentary processes. Unpublished Cand. Sc. Thesis Summary. Geological Institute RAS, Moscow, pp. 25 [In Russian].
Pisarevsky, S.A., Natapov, L.M., 2003. Siberia and Rodinia. Tectonophysics 375, 221–245.
Pisarevsky, S., Natapov, L.M., Donskaya, T.V., Gladkochub, D.P., Vernikovsky, V.A., Pisarevsky, S., Natapov, L.M., Donskaya, T.V., Gladkochub, D.P., Vernikovsky, V.A., 2008. Proterozoic Siberia: a promontory of Rodinia. Precambr. Res. 160, 66–76.
Pisarevsky, S.A., Gladkochub, D.P., Konstantinov, K.M., Mazukabzov, A.M., Stanevich, A.M., Murphy, J.B., Tait, J.A., Donskaya, T.V., Konstantinov, I.K., 2013. Paleomagnetism of Cryogenian Kitoi mafic dykes in South Siberia: implications for Neoproterozoic paleogeography. Precambr. Res. 231, 372–382.
Poller, U., Gladkochub, D.P., Donskaya, T.V., Mazukabzov, A.M., Sklyarov, E.V., Todt, W., 2004. Timing of Early Proterozoic magmatism along the Southern margin of the Siberian Craton (Kitoy area). Fifth Hutton Symposium on the Origin of Granites and Related Rocks 389, 215–225.
Popov, N.V., Likhanov, I.I., Nozhkin, A.D., 2010. Mesoproterozoic granitoid magmatism in the Trans-Angara segment of the Yenisey Range: U-Pb evidence. Dokl. Earth Sci. 431, 418–423.
Postel'nikov, E., 1980. Geosynclinal Evolution of the Yenisey Ridge in the Late Precambrian. Trans. GIN AS USSR, Moscow, pp. 220.
Postnikov, A.A., Terleev, A.A., 2004. Neoproterozoic stratigraphy of the Altai-Sayan folded area. Russ. Geol. Geopys. 45 (3), 295–309.
Postnikov, A.A., Terleev, A.A., Kuznetsov, A.B., Kozhnev, B.B., Nozhkin, A.D., Stanevich, A.M., 2008. The Vorogovka Group of the Yenisey Ridge (New geological and isotope geochemical data), In Sklyarov, E.V. (Ed.), Proceedings of Meeting «Geodynamic evolution of the Central Asian Orogenic Belt lithosphere (from ocean to continent)». V. 11. Irkutsk, IZK SO RAN, pp. 53–55. [In Russian].
Priyatkina, N., Khudoley, A.K., Collins, W.J., Kuznetsov, N.B., Huang, H.-Q., 2016. Detrital zircon record of Meso- and Neoproterozoic sedimentary basins in northern part of the Siberian Craton: characterizing buried crust of the basement. Precambr. Res. 285, 21–38.
Priyatkina, N., Collins, W.J., Khudoley, A.K., Zastrozhnov, D., Ershova, V., Chambarlain, K., Proskurnin, V., Shatsillo, A., 2017. The Proterozoic evolution of northern Siberian Craton margin: a comparison of U-Pb–Hf signatures from sedimentary units of the Taimyr orogenic belt and the Siberian platform. Int. Geol. Rev. 1–27.
Rainbird, R.H., Stern, R.A., Khudoley, A.K., Kropachev, A.P., Heaman, L.M., Sukhorukov, V.I., 1998. U-Pb geochronology of Riphean sandstone and gabbro from southeast Siberia and its bearing on the Laurentia-Siberia connection. Earth Planet. Sci. Lett. 164, 409–420.
Rasskazchikov, A.N., 1958. Geological Map of the USSR. Scale 1: 200 000. Sheet N-47-VIII. VSEGEI, St. Petersburg [In Russian].
Rojas-Agramonte, Y., Kröner, A., Demoux, A., Xia, X., Wang, W., Donskaya, T., Liu, D., Sun, M., 2011. Detrital and xenocrystic zircon ages from Neoproterozoic to Palaeozoic arc terranes of Mongolia: significance for the origin of crustal fragments in the Central Asian Orogenic Belt. Gondwana Res. 19, 751–763.
Romanova, I.V., Vernikovskaya, A.E., Vernikovsky, V.A., Matushkin, N.Y., Larionov, A.N., 2012. Neoproterozoic alkaline magmatism and associated igneous rocks in the western framing of the Siberian craton: petrography, geochemistry, and geochronology. Russ. Geol. Geophys. 53, 1176–1196.
Rosen, O.M., Turkina, O.M., 2007. The oldest Rock assemblages of the Siberian Craton. In: Martin, J. van Kranendonk, Rugh, H.S., Vickie, C.B. (Eds.), Developments in Precambrian Geology. Elsevier, pp. 793–838.
Rosen, O., Condie, K.C., Natapov, L.M., Nozhkin, A., 1994. Archean and early Proterozoic evolution of the Siberian craton: a preliminary assessment. Archean Crustal Evol. 11, 411–459.
Rudnev, S.N., Matukov, D.I., Sergeev, S.A., Serov, P.A., 2006. Late Riphean plagiogranites of Kuznetskii Alatau: composition, age, and sources. Dokl. Earth Sci. 411, 1277–1283.
Rudnev, S.N., Kovach, V.P., Ponomarchuk, V.A., 2013. Vendian-Early Cambrian island-

arc plagiogranitoid magmatism in the Altai-Sayan folded area and in the Lake Zone of western Mongolia (geochronological, geochemical, and isotope data). Russ. Geol. Geophys. 54, 1272–1287.
Rudnick, R., Gao, S., 2003. Composition of the continental crust. Treatise Geochem. 3, 659.
Safonova, I., 2014. The Russian-Kazakh Altai orogen: an overview and main debatable issues. Geosci. Front. 5, 537–552.
Sears, J.W., 2012. Transforming Siberia along the Laurussian margin. Geology 40, 535–538.
Semikhatov, M.A., Serebryakov, S.N., 1983. Siberian Hypostratotype of Riphean Nauka, Moscow, p. 223. [In Russian].
Shenfil', V.Y., 1991. Upper Precambrian of the Siberian Platform. Nauka, Novosibirsk [In Russian].
Sklyarov, E., Gladkochub, D., Mazukabzov, A., Donskaya, T., Stanevich, A., 2002. Geological complexes in the margin of the Siberian Craton as indicators of the evolution of a Neoproterozoic Supercontinent. Russ. J. Earth Sci. 4, 171–186.
Smits, R.G., Collins, W.J., Hand, M., Dutch, R., Payne, J., 2014. A Proterozoic Wilson cycle identified by Hf isotopes in central Australia: implications for the assembly of Proterozoic Australia and Rodinia. Geology 42 (3), 231–234.
Sovetov, J.K., Blagovidov, V.V., 2004. Reconstruction of a basin evolution: example from a Vendian foredeep, a foreland basin in the southwestern Siberian craton. In: Leonov, Yu.G., Volozh, Yu.A. (Eds.), Sedimentary Basins: Structure, Evolution, and Methods of Studies. Nauchny Mir, Moscow, pp. 159–212 [In Russian].
Sovetov, Y.K., Komlev, D.A., 2005. Tillites at the base of the Oselok Group, foothills of the Sayan Mountains, and the Vendian lower boundary in the Southwestern Siberian platform. Stratigr. Geol. Correl. 13, 337–366.
Sovetov, J.K., Kulikova, A.E., Medvedev, M.N., 2007. Sedimentary basins in the southwestern Siberian craton: late Neoproterozoic-Early Cambrian rifting and collisional events. Geol. Soc. Am. Spec. Pap. 423, 549–578.
Spencer, C.J., Cawood, P.A., Hawkesworth, C.J., Prave, A.R., Roberts, N.M., Horstwood, M.S., Whitehouse, M.J., 2015. Generation and preservation of continental crust in the Grenville Orogeny. Geosci. Front. 6, 357–372.
Spencer, C.J., 2016. Hard and fast or soft and slow: rates of crustal reworking and orogenesis in the North Atlantic Region. 35th International Geological Congress Abstracts, abstract #1771.
Stanevich, A.M., Mazukabzov, A.M., Postnikov, A.A., Nemerov, V.K., Pisarevsky, S.A., Gladkochub, D.P., Donskaya, T.V., Kornilova, T.A., 2007. Northern segment of the Paleoasian Ocean: Neoproterozoic deposition history and geodynamics. Russ. Geol. Geophys. 48, 46–60.
Sukhanova, N.V., 1957. Geological Map of the USSR. Scale 1: 200,000. Sheet N-47-IX. VSEGEI, St. Petersburg [In Russian].
Turkina, O.M., Nozhkin, A.D., Bibikova, E.V., Zhuravlev, D.Z., Travin, A.V., 2004. The Arzybei terrane: a fragment of the Mesoproterozoic island-arc crust in the southwestern framing of the Siberian craton. Dokl. Earth Sci. 395, 246–250 [In Russian].
Turkina, O.M., Nozhkin, A.D., Bayanova, T.B., 2006. Sources and formation conditions of Early Proterozoic granitoids from the southwestern margin of the Siberian craton. Petrology 14, 262–283.
Turkina, O.M., Nozhkin, A.D., Bayanova, T.B., Dmitrieva, N.V., Travin, A.V., 2007. Precambrian terranes in the southwestern framing of the Siberian craton: isotopic provinces, stages of crustal evolution and accretion-collision events. Russ. Geol. Geophys. 48, 61–70.
Turkina, O.M., Kapitonov, I.N., Sergeev, S.A., 2013. The isotope composition of Hf in zircon from Paleoarchean plagiogneisses and plagiogranitoids of the Sharyzhalgai uplift (southern Siberian craton): Implications for the continental-crust growth. Russ. Geol. Geophys. 54, 272–282.
Varganov, V.A., Moskalev, V.A., Barmin, V.A., 2010. Geological map of Russian Federation. Scale 1: 1,000,000. Sheet P-46. VSEGEI, Petersburg [In Russian].
Vernikovskaya, A.E., Vernikovsky, V.A., Sal'nikova, E.B., Datsenko, V.M., Kotov, A.B., Kovach, V.P., Travin, A.V., Yakovleva, S.Z., 2002. Yeruda and Chirimba granitoids (Yenisey Ridge) as indicators of Neoproterozoic collisions. Geol. Geofiz. 43, 259–272 [In Russian].
Vernikovskaya, A., Vernikovsky, V., Sal'nikova, E., Kotov, A., Kovach, V., Travin, A., Palesskii, S., Yakovleva, S., Yasenev, A., Fedoseenko, A., 2003. Neoproterozoic Postcollisional Granitoids of the Glushikha Complex, Yenisey Range. Petrologija 11, 48–61 [In Russian].
Vernikovskaya, A., Vernikovsky, V., Sal'nikova, E., Yasenev, A., Kotov, A., Kovach, V., Travin, A., Yakovleva, S., Fedoseenko, A., 2006. Neoproterozoic A-type granites of the Garevka massif, Yenisey Ridge: age, sources, and geodynamic setting. Petrology 14, 50–61.
Vernikovskaya, A.E., Vernikovsky, V.A., Sal'nikova, E.B., Kotov, A.B., Kovach, V.P., Travin, A.V., Wingate, M.T.D., 2007. A-type leucogranite magmatism in the evolution of continental crust on the western margin of the Siberian craton. Russ. Geol. Geophys. 48, 3–16.
Vernikovskaya, A.E., Datsenko, V.M., Vernikovsky, V.A., Matushkin, N.Y., Laevsky, Y.M., Romanova, I.V., Travin, A.V., Voronin, K.V., Lepekhina, E.N., 2013. Magmatism evolution and carbonatite-granite association in the neoproterozoic active continental margin of the Siberian craton: thermochronological reconstructions. Dokl. Earth Sci. 448, 161–167.
Vernikovsky, V., Vernikovskaya, A., Sal'nikova, E., Kotov, A., Chernykh, A., Kovach, V., Berezhnaya, N., Yakovleva, S., 1999. New U-Pb data on the formation of the Predivinsk paleoisland-arc complex (Yenisey Ridge). Geol. Geofiz. 255–259 [In Russian].
Vernikovsky, V.A., Vernikovskaya, A.E., Chernykh, A.I., Sal'nikova, E.B., Kotov, A.B., Kovach, V.P., Yakovleva, S.Z., Fedoseenko, A.M., 2001. Porozhnaya granitoids of the Enisei ophiolite belt: indicators of neoproterozoic events on the Enisei ridge. Dokl. Earth Sci. 381, 1043–1046 [In Russian].
Vernikovsky, V.A., Vernikovskaya, A.E., Kotov, A.B., Sal'nikova, E.B., Kovach, V.P., 2003. Neoproterozoic accretionary and collisional events on the western margin of the Siberian craton: new geological and geochronological evidence from the Yenisey Ridge. Tectonophysics 375, 147–168.
Vernikovsky, V.A., Vernikovskaya, A.E., Wingate, M.T.D., Popov, N.V., Kovach, V.P., 2007. The 880–864 Ma granites of the Yenisey Ridge, western Siberian margin: geochemistry, SHRIMP geochronology, and tectonic implications. Precambr. Res. 154, 175–191.
Vernikovsky, V.A., Vernikovskaya, A.E., Sal'nikova, E.B., Berezhnaya, N.G., Larionov, A.N., Kotov, A.B., Kovach, V.P., Vernikovskaya, I.V., Matushkin, N.Y., Yasenev, A.M., 2008. Late Riphean alkaline magmatism in the western margin of the Siberian Craton: a result of continental rifting or accretionary events? Dokl. Earth Sci. 419, 226–230.
Vernikovsky, V.A., Kazansky, A.Y., Matushkin, N.Y., Metelkin, D.V., Sovetov, J.K., 2009. The geodynamic evolution of the folded framing and the western margin of the Siberian craton in the Neoproterozoic: geological, structural, sedimentological, geochronological, and paleomagnetic data. Russ. Geol. Geophys. 50, 380–393.
Vernikovsky, V.A., Metelkin, D.V., Vernikovskaya, A.E., Matushkin, N.Y., Kazansky, A.Y., Kadilnikov, P.I., Romanova, I.V., Wingate, M.T.D., Larionov, A.N., Rodionov, N.V., 2016. Neoproterozoic tectonic structure of the Yenisey Ridge and formation of the western margin of the Siberian craton based on new geological, paleomagnetic, and geochronological data. Russ. Geol. Geophys. 57, 47–68.
Vervoort, J.D., Blichert-Toft, J., 1999. Evolution of the depleted mantle: Hf isotope evidence from juvenile rocks through time. Geochim. Cosmochim. Acta 63, 533–556.
Volobuev, M.I., Zykov, S.I., Stupnikova, N.I., 1976. Geochronology of Precambrian formations of the Sayan-Yenisei region of Siberia. In: Vinogradov, A.P. (Ed.), Topical Problems of the Modern Geochronology. Nauka, Moscow, pp. 96–123 [In Russian].
Yang, J.-H., Wu, F.-Y., Wilde, S., Xie, L.-W., Yang, Y.-H., Liu, X.-M., 2007. Tracing magma mixing in granite genesis: in situ U-Pb dating and Hf-isotope analysis of zircons. Contrib. Mineral. Petrol. 153, 177–190.
Zuev, V.K., Perfilova, O.Yu., 2012. Geological Map of Russian Federation. Scale 1:1,000,000. Sheet O-47. VSEGEI, Petersburg [In Russian].